Quaternary Science Reviews 93 (2014) 106–124

Contents lists available at ScienceDirect

Quaternary Science Reviews

journal homepage: www.elsevier.com/locate/quascirev

Chronology of Quaternary coastal aeolianite deposition and the drowned shorelines of southwestern Western Australia – a reappraisal

B.P. Brooke [a,*], J.M. Olley [b], T. Pietsch [b], P.E. Playford [c], P.W. Haines [c], C.V. Murray-Wallace [d], C.D. Woodroffe [d]

[a] Coastal Marine and Climate Hazards Group, Geoscience Australia, Canberra, ACT 2601, Australia
[b] Australian Rivers Institute, Griffith University, Nathan, QLD 4111, Australia
[c] Geological Survey of Western Australia, East Perth, WA 6004, Australia
[d] School of Earth & Environmental Sciences, University of Wollongong, NSW 2522, Australia

ARTICLE INFO

Article history:
Received 30 December 2013
Received in revised form
3 April 2014
Accepted 5 April 2014
Available online 4 May 2014

Keywords:
Optically Stimulated Luminescence
OSL
Coastal evolution
Marine carbonate sediment
Eolianite
Pleistocene sea levels
Tamala Limestone
Aeolianite

ABSTRACT

Aeolianite successions of low-gradient continental margins commonly show complex records of coastal dune deposition linked to a wide range of sea-level positions and climatic periods of the middle and late Pleistocene, recording both regional and broader-scale drivers of sediment production, coastal dune development and landform preservation. To better characterise the general pattern of sedimentation that occurs over Quaternary glacial–interglacial cycles on low-gradient, temperate carbonate continental shelves we examine the morphology, stratigraphy and age of aeolianite deposits in the Perth region, Western Australia. This includes an analysis of well-defined drowned coastal landforms preserved on the adjacent shelf. New and previously published optical ages provide a preliminary timeframe for the deposition of aeolianite in the Perth region and on Rottnest Island, 17 km offshore. An extensive aeolianite ridge near Perth, representing a former barrier, has Optically Stimulated Luminesence (OSL) ages that range from 120 ± 12 to 103 ± 10 ka (MIS 5e–5a in the context of associated age uncertainties). OSL ages for an exposure in the same ridge 2.5 km inland, record the onlap of much older aeolianite, OSL age 415 ± 70 ka, by shell-rich estuarine beds, OSL age 290 ± 30 ka. A further 5.5 km inland from the coast, two thick aeolianite units, separated by a well-developed palaeosol, have stratigraphically consistent OSL ages of 310 ± 30 and 155 ± 20 ka. In contrast, aeolianite units that form the northern coast of Rottnest Island have OSL ages of 77 ± 12 ka and 27 ± 5 ka. The new OSL ages and previously reported TL and U/Th ages indicate that the bulk of the island comprises dunes deposited around the end of the Last Interglacial *sensu lato* (MIS 5a–4) and during the Last Glacial (MIS 4–2), accumulating over a Last Interglacial coral reef and basal calcarenite. Drowned barrier and dune landforms preserved on the adjacent continental shelf reveal that barriers were formed during periods of intermediate sea level (e.g. MIS 3) and significant dune mobility occurred when the shelf was subaerially exposed. The pattern of shelf sedimentation discernible in the Perth region – large-scale coastal carbonate dune deposition during periods of high and intermediate sea level and reactivation during glacial lowstands – is largely consistent with published stratigraphic and age data for large-scale aeolianite deposits on other low-gradient carbonate shelves. Based on these data, a general model is proposed for the cycle of Quaternary sedimentation and landform evolution that occurs on these shelves, which are dynamic sedimentary environments with coastal landforms and sedimentary successions that are very sensitive to erosion and sediment reworking.

1. Introduction

Aeolianite coasts have provided many fundamental insights into coastal sedimentation and landform development during Quaternary glacial cycles. Classic sites such as the aeolianite islands of

* Corresponding author. Tel.: +61 2 62499434; fax: +61 2 62499920.
E-mail address: Brendan.Brooke@ga.gov.au (B.P. Brooke).

http://dx.doi.org/10.1016/j.quascirev.2014.04.007

Bermuda and the Bahamas have well-preserved relict coastal dune landforms that have recorded the mode and rate of Quaternary coastal landform evolution and marine biogenic carbonate sediment production during the past few glacial–interglacial cycles, when sea level was high enough to flood the surrounding shallow shelves (Vacher et al., 1995; Carew and Mylroie, 1997; Kindler and Hearty, 1997; Vacher and Rowe, 1997). The gently uplifting Coorong Coastal Plain of South Australia preserves an even more extensive series of relict coastal barriers that formed marginal to a broad continental shelf (Murray-Wallace, 2002). These barriers developed with the input of fluvial and marine carbonate sediment to the coast during successive interglacial and glacial periods over at least the past 1 million years (Murray-Wallace et al., 2001).

Studies of several continental aeolianite coasts commonly show a more complex record of coastal dune deposition linked to a wide range of sea-level positions and climatic periods of the middle and late Pleistocene (Brooke, 2001), including the South African eastern (Porat and Botha, 2008) and southern coasts (Bateman et al., 2004, 2011; Carr et al., 2007), Carmel coast of Israel (Frechen et al., 2004; Sivan and Porat, 2004), Victorian coast of Australia (Gardner et al., 2006) and Mallorca (Fornos et al., 2009). In addition to dune emplacement during the last couple of interglacials, these deposits include units emplaced through the aeolian reworking of coastal and shelf sediment during periods of low sea level (e.g. Sivan and Porat, 2004; Porat and Botha, 2008) and under a more arid and windy climate than present (Porat and Botha, 2008; Fornos et al., 2009; Playford et al., 2013), or with fluctuations in sea level during interstadials (Bateman et al., 2004, 2011; Gardner et al., 2006). Aeolianite on these coasts appears to record both regional and broader-scale drivers of coastal dune mobility and accumulation. To better understand these Quaternary shelf sediment systems, information is required on the stratigraphy and age of coastal deposits and landforms that formed on the adjacent continental shelves during periods when sea level was lower than present (e.g., Brooke et al., 2010; Bateman et al., 2011; Cawthra et al., 2012). In particular, preserved morphological information on drowned shelf deposits can provide new insight into the glacial–interglacial cycle of carbonate shelf sedimentation, during which coastal deposits may accumulate with the direct input to the coast of carbonate produced offshore; or with the reworking of subaerially exposed shelf sediment during periods of low sea level.

This study examines a range of new and previously published age data for the aeolianite deposits around Perth, Western Australia. The data are set within a regional morphostratigraphic context provided by a high-resolution digital elevation model of the coastal plain and adjacent continental shelf, which reveals a number of relict shorelines. We examine the timing of deposition of the aeolianite in relation to the glacio-eustatic sea-level record and the morphology and elevation of relict shorelines. A conceptual model of Quaternary carbonate production and aeolianite formation over a full glacial–interglacial cycle is proposed that may also be applicable to other carbonate continental shelves.

2. Regional setting

Aeolianite along the coast of southwestern Australia is known as the Tamala Limestone, a Pleistocene lithostratigraphic unit of the Perth and Carnarvon Basins (Playford et al., 1976, 2013), and represents a vast accumulation of Pleistocene marine carbonate sediment (Fig. 1; Mayer, 2008). The great extent, composition and general stratigraphy of these deposits, including exposures in what is now the Perth region, were first described in 1801 by geologists on the French scientific expedition of the coast of western and southern Australia, led by Nicholas Baudin (Mayer, 2008). Since then several exposures of the Tamala Limestone have been examined in which dune, palaeosol and subordinate shallow-marine units record cycles of coastal sedimentation (Fairbridge and Teichert, 1953; Playford et al., 1976; Murray-Wallace and Kimber, 1989; Kendrick et al., 1991, 1997; Price et al., 2001; Hearty, 2003; Gozzard, 2007; Hearty and O'Leary, 2008; Playford et al., 2013).

Perth has a Mediterranean climate, with hot dry summers (average max. 31 °C, min. 19 °C; average monthly rainfall 12 mm) and cool relatively wet winters (average max. 19 °C, min. 8 °C; average monthly rainfall 132 mm) (Bureau of Meteorology, 2012). There is an energetic wind regime on the coast (average monthly 3 pm wind speed, 12.5–19.5 km/h), dominated by onshore wind from the SW–W (Bureau of Meteorology, 2012). The orientation of large-scale dune foreset beds measured at the aeolianite exposures described below record deposition under wind from similar onshore directions. The Perth coast forms the margin of the broad (up to 50 km wide) Rottnest Shelf, which receives very little terrestrial sediment and is dominated by marine biogenic carbonate sediment (Collins, 1988). The shelf experiences a high-energy south to southwesterly swell, with a mean deep-water wave height of 2–3 m and period of 10–14 s. Shelfal waters are subtropical (16–20 °C) and influenced by the warm, low-nutrient waters of the southerly flowing Leeuwin Current (Collins, 1988), with a micro-tidal regime (<2 m range).

The Perth coast, part of the Swan Coastal Plain, comprises three major aeolianite ridges, with 20–40 m of relief, that run semi-parallel to the shoreline and rise in elevation with distance from the coast (Fig. 2; Playford et al., 1976; Playford, 1988, 1997; Gozzard, 2007; Brooke et al., 2010). A chain of aeolianite islands and reefs extend out from the Perth coast (Fig. 2). These features include a series of submerged ridges that are the remnants of a recurved aeolianite coastline that existed when sea level was more than 20 m lower than present (Fig. 2; Playford, 1988, 1997). Further offshore, a less well defined linear structure extends along most of the outer Rottnest Shelf and probably represents the erosional remnant of a drowned shoreline barrier (James et al., 1999; Brooke et al., 2010). This feature rises 5–15 m above the adjacent seabed, is approximately 2–4 km wide and sits 60–50 m below sea level (Fig. 2B). It merges with the western margin of Rottnest Island, while south of the island the features becomes less distinct (Brooke et al., 2010).

Several sections of middle and late Pleistocene dune units have been studied in the Tamala Limestone near Perth and on the nearby islands (Price et al., 2001; Hearty, 2003; Hearty and O'Leary, 2008), with occasional outcrops of Last Interglacial coral reef (Szabo, 1979; Kendrick et al., 1991; Stirling et al., 1998) and middle Pleistocene and Last Interglacial mollusc-rich estuarine beds (Hewgill et al., 1983; Murray-Wallace and Kimber, 1989; Kendrick et al., 1991). The elevation of reliably dated estuarine and reef deposits, in particular the robustly dated Last Interglacial (MIS 5e) coral reef at Fairbridge Bluff on Rottnest Island (Szabo, 1979; Stirling et al., 1995, 1998) suggest that the area has been tectonically stable since at least the later part of the middle Pleistocene (Kendrick et al., 1991). However, examples of neotectonism in the region have been noted by Playford et al. (2013), who record faulting that post-dates deposition of part of the Tamala Limestone near Jurien, 220 km north of Perth, raising the possibility of faulting in the late Pleistocene or early Holocene.

The chronology of the ubiquitous aeolianite of the Tamala Limestone is relatively poorly resolved (Kelletat, 1991; Price et al., 2001; Hearty, 2003; Hearty and O'Leary, 2008). Whole-rock amino acid racemisation (AAR) age estimates of aeolianite near Perth are middle Pleistocene and Last Interglacial, whereas age estimates for aeolianite on Rottnest Island predominantly lie within the period from marine oxygen isotope substages (MIS) 5c to 5a (Hearty, 2003). In contrast, thermoluminescence (TL) ages of the

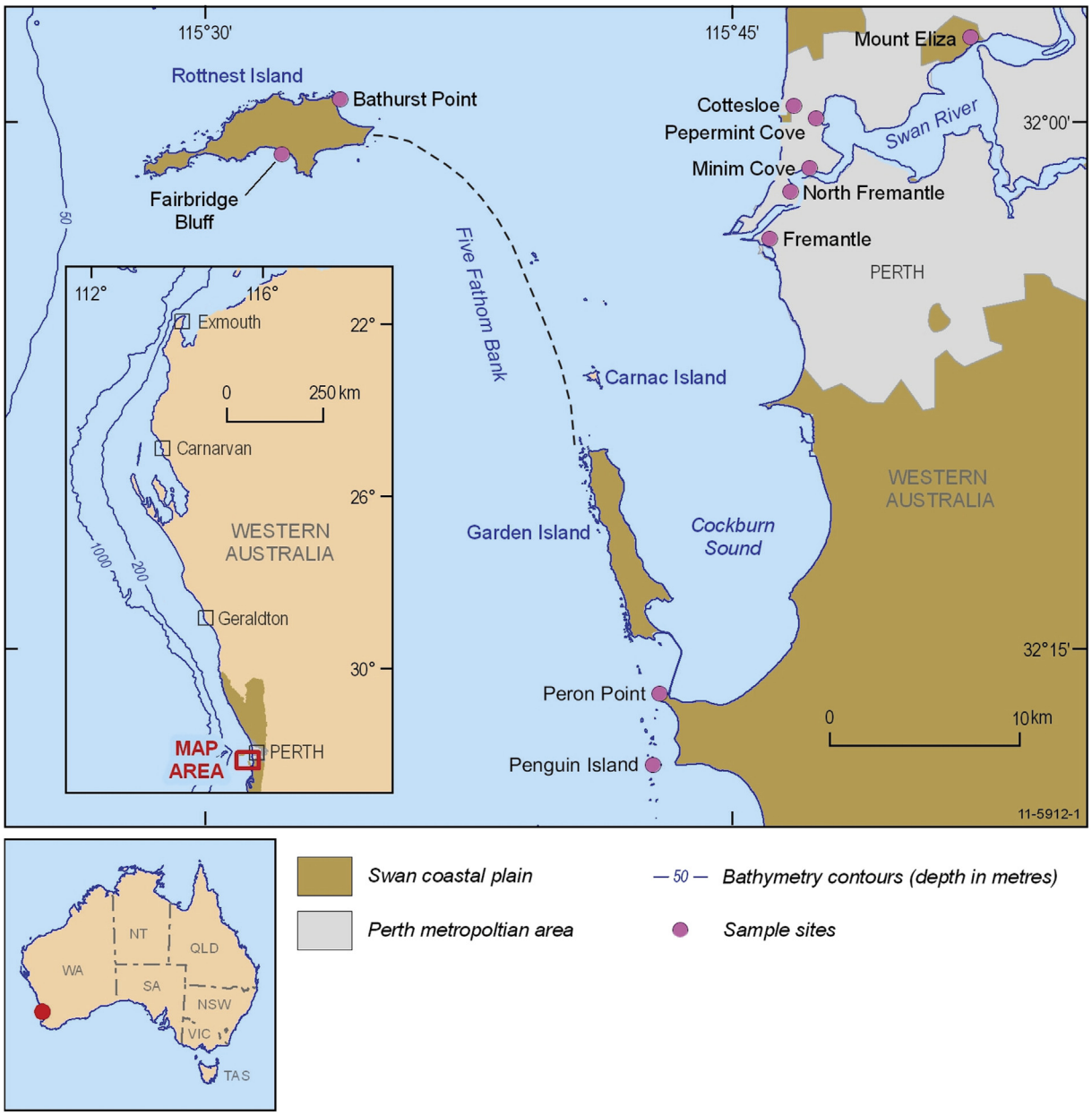

Fig. 1. Perth and the Swan Coastal Plain on the southwest coast of Western Australia. Sites examined in this study and other locations discussed in the text are shown.

quartz component of several of the same aeolianite units suggest deposition of dunes on the mainland coast and nearby Penguin Island during the period from MIS 5c to 5a, and at Rottnest Island in MIS 3 and just prior to or during the Last Glacial, MIS 3–2 (Price et al., 2001). In this paper the AAR and TL ages are compared with new OSL ages for the same units, which generally agree with the previously derived TL chronology.

3. Methods

Stratigraphic sections were examined and samples collected at exposures of aeolianite and shallow-marine calcarenite around Perth and at Bathurst Point on Rottnest Island (Fig. 1; Table 1). Sediment characteristics were assessed in the field or under binocular microscope and the proportion of calcium carbonate in samples was determined using the 'bomb' gas evolution method (Muller and Gastner, 1971). For all but one of the sample sites (Fremantle, F01), AAR and TL ages have previously been reported for at least one of the dune or shallow-marine units sampled (Table 2). OSL samples are from beds that have been buried by overlying sediment to depths ranging from 4 to 30 m (Table 1). At the OSL sampling sites, the least-altered areas of outcrops were targeted, weathered sediment was removed from the exposure and then a hole was augered into the face of the outcrop to a depth of 0.7–1.0 m, depending on the hardness of the limestone. Light was excluded from the hole as the OSL samples were collected.

3.1. Elevation data analysis

A regional spatial framework for the sample sites is provided by a digital elevation model (DEM) that was generated from merged high-resolution topographic and bathymetric data for the region. Spatial data analysis methods are described in detail in Brooke et al. (2010). In summary, the DEM presented here integrates a range of

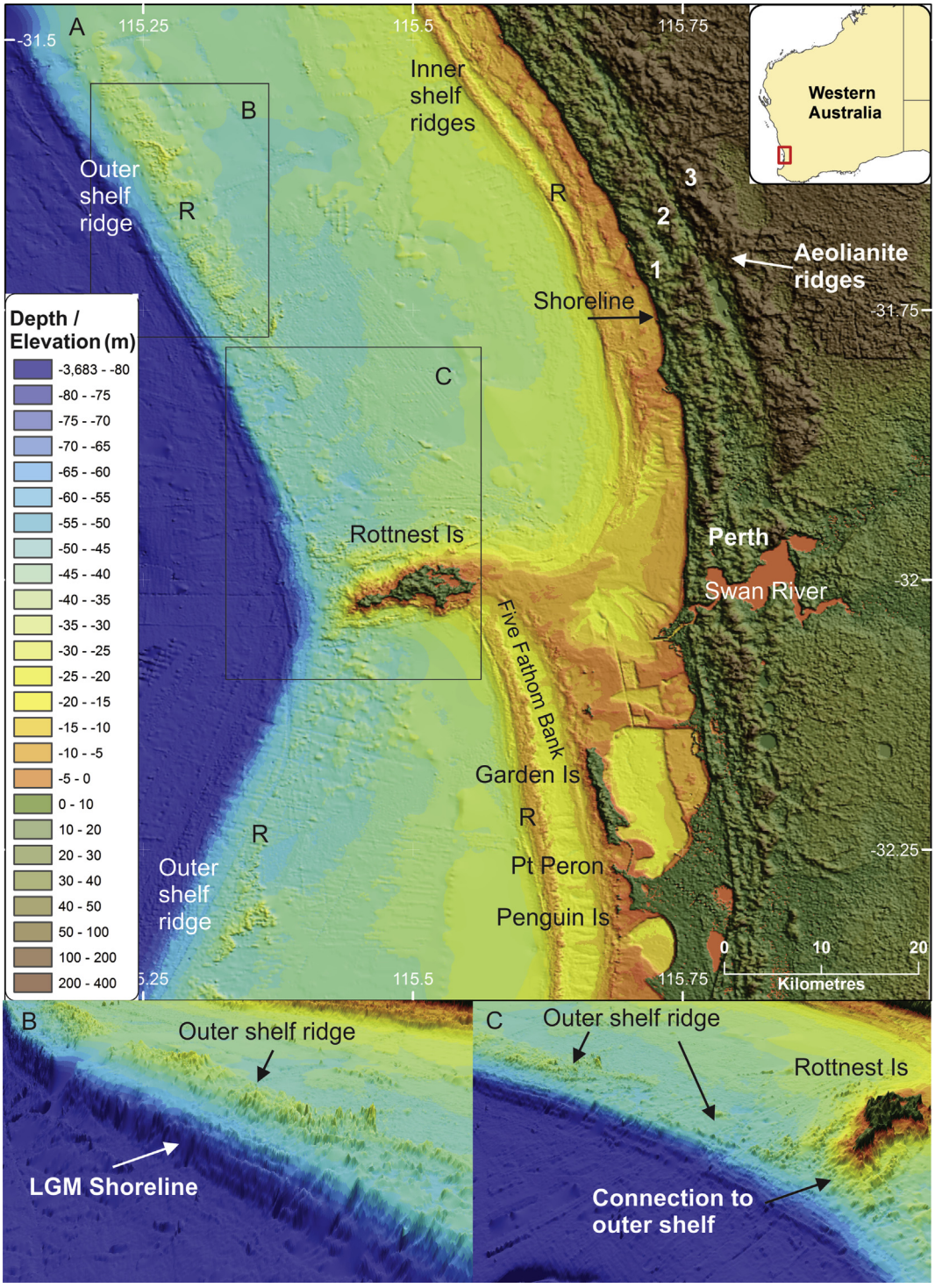

Fig. 2. Digital relief models of the Rottnest Shelf (dark blue to orange) and Swan Coastal Plain (dark green to brown) around Perth. A: The image is a combination of high-resolution bathymetric and topographic data (described in text). Aeolianite ridges of the Tamala Limestone on the Swan Coastal Plain (1, 2, 3) and relict submerged ridges on the shelf (R) are clearly visible. The submarine ridges on the inner shelf are more spatially compressed N of Rottnest Is. The ridge on the outer shelf is well-defined in the area to the NW of Rottnest Is. B: 3D-view enlargement of the outer shelf ridge NW of Rottnest Is. C: 3D-view enlargement of the outer shelf ridge near Rottnest Is. The submarine extension of Rottnest Is (land area is dark green/brown; subtidal is orange and yellow) connects with the outer shelf ridge. The deep water (dark blue) extends W to the head of the Perth Canyon. (For interpretation of the references to colour in this figure legend, the reader is referred to the web version of this article.)

bathymetric and topographic data acquired by the governments of Western Australia and Australia, as described in Brooke et al. (2010), and additional high-resolution multibeam echosounder bathymetric data acquired during surveys of *RV Southern Surveyor*, the Australian National Facility research vessel, between 2008 and 2012. The bathymetric and topographic datasets were converted to WGS84 and Mean Sea Level (MSL) datums. They were imported into ArcGIS v10, and regridded to a 50 m cell size (vertical resolution ~0.50 m). This combined dataset was enhanced with a NE sun-angle filter and pseudocolour lookup table to highlight

Table 1
OSL samples from units of the Tamala Limestone around Perth and Rottnest Island.

Sample no.	Location	Coordinates (degrees)	Facies	Elevation + MLW (m)	Sample burial depth (m)	% $CaCO_3$
CB02	Cottesloe Beach: shoreline cliff	S 31.9978 E 115.751	Gravelly beach foreshore beds.	2	5	29
CB01	Cottesloe Beach: shoreline cliff	31.9985 115.751	Medium grain dune foreset beds.	6	2	56
F01	North Fremantle: cutting, Sterling Hwy	32.03325 115.752	Medium-fine grain dune topset beds.	6	5	52
RH01	Arthur Head, Fremantle: cliff at RoundHouse	32.05661 115.741	Medium-fine grain steeply dipping dune foreset beds.	3.5	5	86
MC02	Minim Cove: W wall of disused quarry	32.0227 115.768	Medium-fine grain dune foreset beds.	30	6	49
MC01	Minim Cove: cliff exposure in N bank of Swan Estuary	32.02371 115.77	Gravely, shell-rich, subtidal beds.	2	4	29
PG01	Peppermint Grove: cliff adjacent to Swan Estuary	31.99612 115.772	Gravely, shell-rich, subtidal beds.	3	4.5	33
PG02	Peppermint Grove: cliff adjacent to the Swan Estuary	31.99536 115.772	Medium-fine grain dune foreset beds.	10.5	4.5	30
KP01	Kings Park Perth: cliff exposure above Kennedy Fountain.	31.96239 115.84301	Medium-fine grain dune foreset beds.	10	30	48
KP02	Kings Park Perth: exposure ~10 m above KP01	31.96211 115.84213	Medium-fine grain dune foreset beds.	30	5	–
RI02	Cliff exposure at Bathurst Point	31.9899 115.5423	Medium-fine grain, dune foresets, below palaeosol.	2.5	15.5	94
RI01	Cliff exposure at Bathurst Point	31.9899 115.5422	Medium-fine grain dune foresets, above palaeosol.	10	8	96

structures. In total, the data cover an area of continental shelf and coastal plain of approximately 7400 km^2.

3.2. OSL methods

OSL dating was undertaken at the CSIRO OSL Laboratory, Canberra, using methods and instrumentation described in detail in Olley et al. (2004a,b). In brief, samples were prepared using standard procedures (e.g. Aitken, 1998) designed to isolate pure extracts of 180–212 μm light safe quartz grains. Single grain OSL measurements were made using a Risø TL/OSL DA-15 instrument described in Botter-Jensen et al. (2000) and applying the modified single-aliquot regenerative-dose protocol of Olley et al. (2004a,b), which incorporates an IR wash prior to each OSL readout. Grains were rejected if they met one or more of the following rejection criteria: failure to produce an OSL signal in response to the first ~1 Gy test dose; having OSL decay curves that did not reach background after 1 s of laser stimulation; having growth curves with observable recuperation indicated by zero dose points with a sensitivity-corrected OSL not within 1σ of zero; having recycling ratios not consistent with unity at 1σ; having regeneration points that either have individual uncertainties >15% or lie more than 2σ

Table 2
Previously published age estimates for the dune and shallow-marine units dated by OSL in this study.

Location & Facies	Past age estimates[a]	New OSL ages (ka) & Sample no.	Stratigraphic features
Cottelsoe Beach: beach foreshore beds	TL: 78 ± 9 AAR w-r: MIS 5e	105 ± 9 CB02	Beds sit up to +2 m MLW; moderately to weakly diagenetically altered; a few *in-situ* corals at base.
Cottesloe Beach: dune foreset beds	TL: 79 ± 9	114 ± 9 CB01	Moderately to weakly altered; *terra rossa* palaeosol cap.
North Fremantle: dune topset beds	NA	120 ± 12 F01	Moderate diagenetic alteration, abundant fine rhizoliths.
Fremantle, Arthur Head (Fort): dune foreset beds	TL: 72 ± 5 AAR w-r: MIS 11	103 ± 10 RH01	Moderately altered; solution/soil pipes & calcrete column; *terra rossa* palaeosol cap.
Minim Cove: dune foreset beds	MIS5e	115 ± 10 MC02	Moderately to weakly altered; *terra rossa* palaeosol cap.
Minim Cove:shallow subtidal shell-rich beds	ESR: MIS 5e AAR molluscs: MIS 5e AAR w-r: MIS 5e	104 ± 9 MC01	Weakly indurated, very well preserved mollusc-rich beds sit +2–4 m MLW; herringbone bedding.
Peppermint Grove: shallow subtidal shell-rich beds	ESR: MIS 7 AAR molluscs: MIS 7 AAR w-r: MIS 7–9?	290 ± 29 PG01	Subtidal beds, well preserved molluscs; onlaps highly altered calcarenite.
Peppermint Grove: dune foreset beds	NA	415 ± 70 PG02	Moderately to highly altered; large solution pipes.
Kings Park: dune foreset beds	TL: >422 ka AAR w-r: >MIS 11	310 ± 30 KP01	Moderately to highly altered; soil pipes; *terra rossa* palaeosol.
Rottnest Is, Bathurst Pt: dune foreset beds.	TL: 67 ± 9 AAR w-r: MIS 5e	77 ± 12 RI02	Moderate to low alteration; palaeosol cap.
Rottnest Is, Bathurst Pt: dune foreset beds.	TL: 20 ± 2 AAR w-r: MIS 5c–5a	27.0 ± 4.5 RI01	Moderate to low alteration.

[a] TL ages: Price et al. (2001); ESR (Electron Spin Resonance) age estimates: Hewgill et al. (1983); AAR mollusc ages: Murray-Wallace and Kimber (1989); AAR w-r (whole-rock) age estimates: Hearty (2003), Hearty and O'Leary (2008).

above or below the fitted curve; having growth curves that saturated below or near the Natural. Five hundred single grains were analysed for samples RI01, RI02, KP01 and CB01. For each of the remaining samples, one thousand grains were analysed. Acceptance ratios averaged 9% across all samples. Burial doses and overdispersion parameters were calculated using the central age model of Galbraith et al. (1999), with central values for the multiple dose components apparent in samples PG01 and PG02 determined using the finite mixture model (Roberts et al., 2000; Galbraith, 2005). Lithogenic radionuclide activity concentrations in the OSL samples were determined using high-resolution gamma spectrometry (Murray et al., 1987), with dose rates calculated using the as measured water contents and the conversion factors of Stokes et al. (2003). The β-attenuation factors were taken from Mejdahl (1979). Cosmic dose rates were calculated from Prescott and Hutton (1994), using, in the first instance, the observed burial depths.

4. Results

4.1. Sediments

Sediment samples comprise predominantly medium-grained carbonate–quartz sand, with 30–96% calcium carbonate, which is typical of aeolianite and shallow-marine deposits in this region (Milnes et al., 1987; Hearty and O'Leary, 2008). The carbonate fraction is dominated by fragments of molluscs, red algae and foraminifera, which represent a typical temperate heterozoan assemblage, similar to the modern shelf sediments found offshore from Perth (Collins, 1988). The quartz grains are predominantly well-rounded indicating long periods of mobility. The shallow-marine units include beds of bivalve shells and bioclastic sandy gravel, coral-rich gravel, and quartz–carbonate sand (Table 1; Figs. 3 and 4).

4.2. OSL laboratory data

Concentrations of ^{238}U, ^{226}Ra and ^{210}Pb are consistent with secular disequilibrium in all samples (Table 3). Both samples from Rottnest Island (RI01, RI02) have a ^{238}U excess, which is commonly found in coastal environments. The dose rates presented here have been calculated assuming ^{238}U/^{230}Th equilibrium. Using a ^{230}Th/^{226}Ra equilibrium assumption instead would result in a <1% increase in final calculated age. One sample from Kings Park (KP02) has a ^{210}Pb excess consistent with enrichment via atmospheric fallout. However, the subsequently presented calculated age for Kings Park does not support this conclusion.

Single grains of quartz which did not meet any of the rejection criteria proved to be reliable dosimeters free of malign behaviour (Fig. 5A, B). Growth curve saturation varied across a wide range within each sample, from below the burial dose (except in the case of RI01) to very much above it. This variability in growth curve saturation meant that we avoided problems associated with the mis-identification of spurious dose concentrations associated with a constant growth-curve saturation point.

Where it could be calculated, the over-dispersion parameter (σd, Table 4) is below 22%, which has previously been argued to be the upper limit for well-bleached samples (Olley et al., 2004a,b). However, two samples (e.g. PG01, PG02) appear to contain a secondary population of contaminant grains, either due to sampling error, or dose-rate heterogeneity (Fig. 5B; due, perhaps, to the input of secondary cements or leaching of radionuclides during diagenesis). The calculated OSL ages are reported with 1 sigma uncertainties throughout the paper.

4.3. Aeolianite morphology, stratigraphy and age

The DEM provides an accurate regional-scale representation of the shore-parallel ridges that extend along the coastal plain and similar structures on the inner and outer continental shelf, incorporating all areas influenced by cyclical movements of sea level during the Quaternary (Fig. 2). At least three aeolianite ridges are discernible on the coastal plain north of the Swan River (Fig. 2A). The lower reach of the river has cut into the aeolianite, providing key exposures in the western (seaward) ridge at Kings Park, Peppermint Grove and Minim Cove (Fig. 3). The OSL ages for samples from superposed units at Kings Park, Peppermint Grove, Minim Cove, Cottesloe Beach and Rottnest Island are consistent with their stratigraphic positions (Fig. 3).

4.4. Kings Park, central Perth

At Kings Park, two dune units were sampled (Figs. 3A and 4A). The lower unit (A1) comprises dune foreset beds (E to NE dip orientation) and has a TL age of >422 ka (Price et al., 2001). This unit thins to the east and is capped by a thick (up to 2 m) reddish brown palaeosol. The upper dune unit (A2) unconformably overlies the palaeosol and comprises thick, steeply dipping foreset strata (25–30° dip), with a similar dip strike (NE–SE). The upper unit is capped by a soil horizon with strong weathering features such as solution tubes and soil-filled pipes (Fig. 4A). The OSL age of the basal dune unit, 310 ± 30 ka (MIS 9; KP01, Table 4), is significantly younger than the TL age estimate (>422 ka). The OSL age of the overlying aeolianite, 155 ± 20 ka (KP02), suggests deposition during the glacial period represented by MIS 6.

4.5. Peppermint Grove and Minim Cove

At both sites, exposures of gravelly, mollusc-rich estuarine shell beds and aeolianite were examined in cliff exposures in or adjacent to the northern bank of the Swan River estuary (Figs. 3 and 4; more detailed descriptions of exposures at these sites are provided in Gozzard (2007)). The assemblage of molluscs at both sites includes the intertidal-to-shallow subtidal species *Anadara trapezia*, *Katelysia scalarina* and *Katelysia rhytiphora*. The Peppermint Grove 'boat shed' section (adjacent to Scott's College boat shed and jetty; Figs. 3B and 4B) records a lower-estuarine depositional environment (Kendrick et al., 1991) and has been dated as Penultimate Interglacial, MIS 7 (ESR ages, Hewgill et al., 1983; AAR mollusc ages, Murray-Wallace and Kimber, 1989). The estuarine beds onlap heavily cemented calcarenite and are overlain by dune cross-beds. The top of the estuarine and dune units exhibits weakly developed palaeosol horizons (Fig. 3B). Around 40 m further north, subtidal estuarine calcarenite also crop out a few metres above the shoreline (Gozzard, 2007). Around 150–300 m north of the boat shed, and 10–15 m above the shoreline, there are large exposures of heavily cemented dune foreset cross-beds, up to 10 m thick, emplaced under easterly wind (Figs 3B and 4Bii). This thick dune unit is a major structural element of the aeolianite ridge that runs through the site and most likely represents the basal unit of the succession exposed at Peppermint Grove. Overall, the sections examined at Peppermint Grove record the erosion of the aeolianite ridge by the Swan River, subsequent estuarine sedimentation and then a phase of dune deposition (Fig. 3G).

As noted, the OSL ages for Peppermint Grove are problematic due to two distinct dose components within the single grain D_e population for these two samples (Table 4; Fig. 5B). Nonetheless, the OSL age estimates (using a two component finite mixture model) for the thick aeolianite unit (PG02, 220 ± 20/415 ± 70 ka) indicate a middle Pleistocene age. The OSL age estimate for the

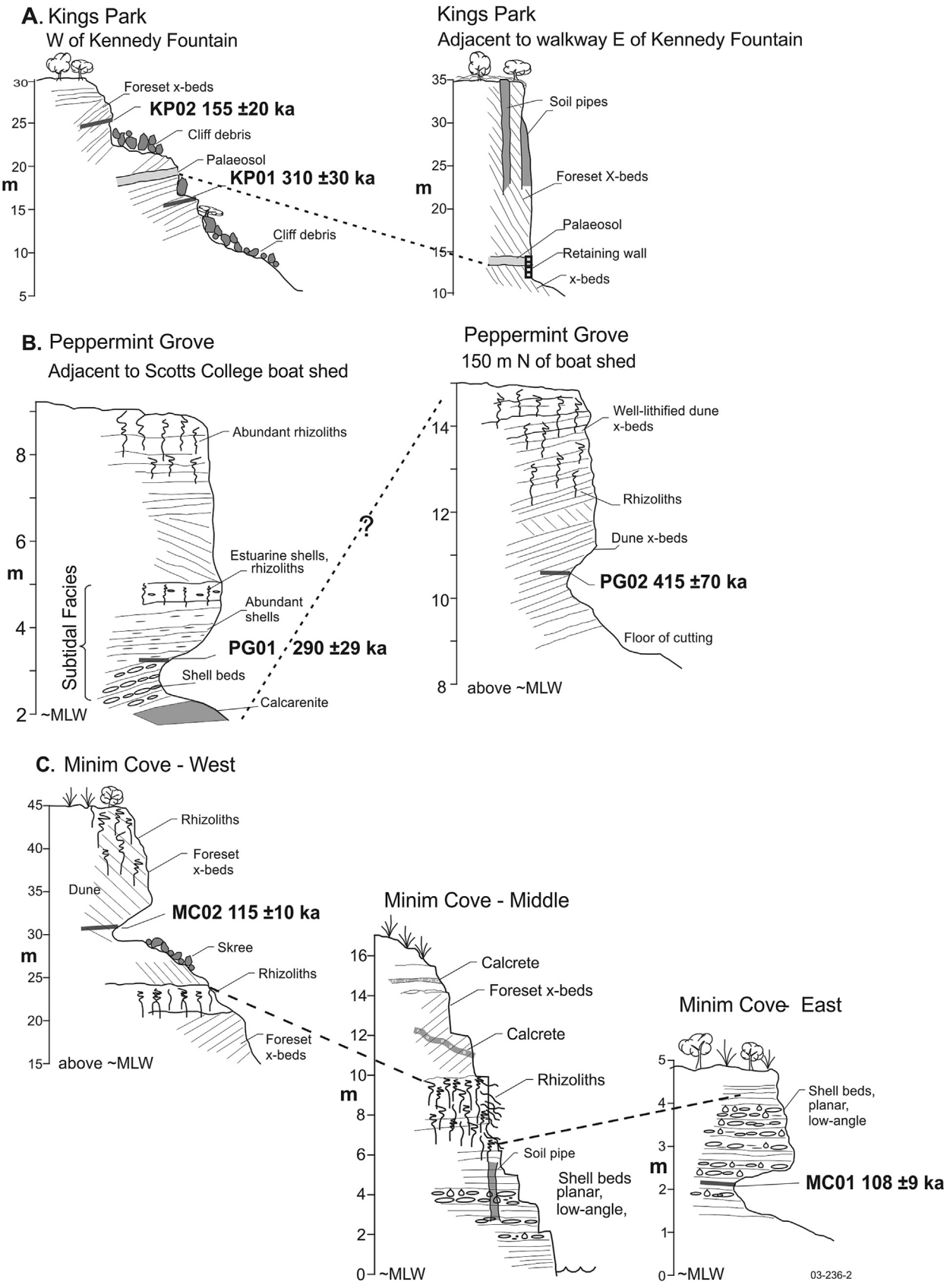

Fig. 3. Measured sections of the Tamala Limestone around Perth (A–E) and on Rottnest Island (F). The position and age of the OSL samples are indicated (MLW – approximate position of Mean Low Water as observed in the field). An overview of the Tamala Limestone stratigraphy at the sample areas is shown in G, which includes Fairbridge Bluff, the location of a LIG coral reef (Stirling et al., 1995).

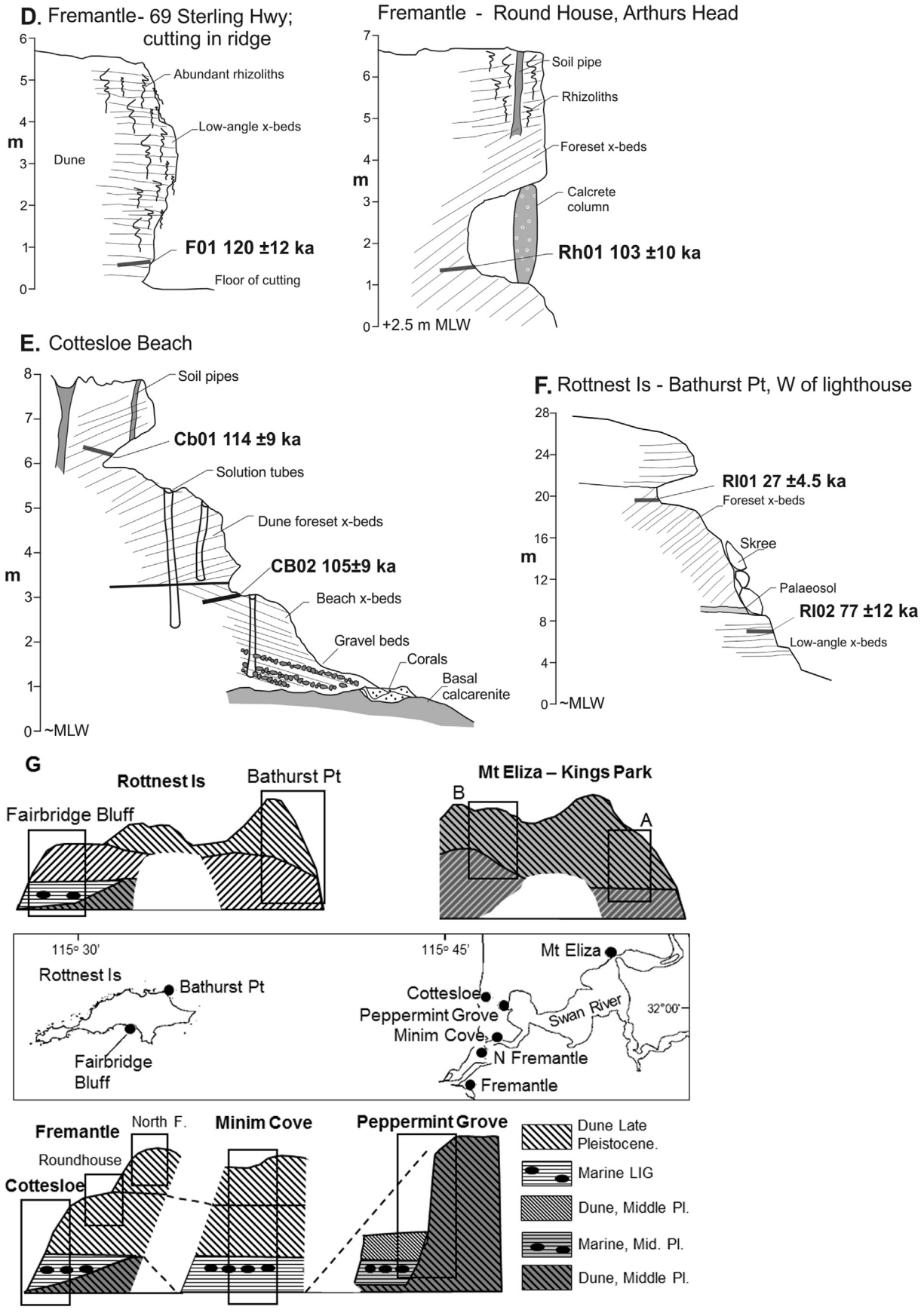

Fig. 3. (*continued*).

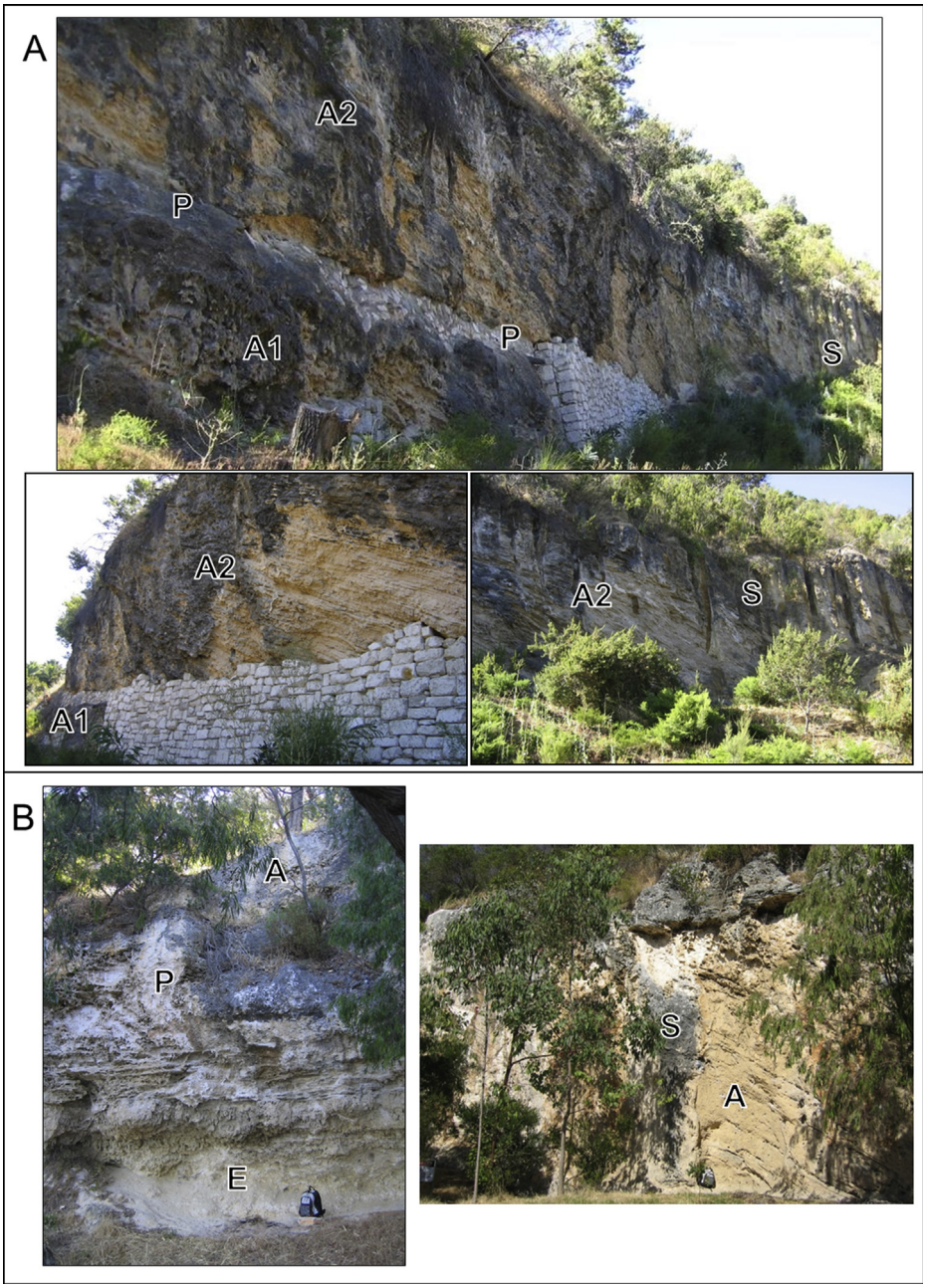

Fig. 4. Photographs of the sections examined at Perth and Rottnest Island. A: Kings Park. Fig. Ai (top): Aeolianite exposures adjacent to the park's southern walkway. Stabilization work has reinforced the base of the cliff where the palaeosol (P) crops out. The palaeosol sits between two aeolianite units (A1 and A2, both sampled for OSL). Fig. Aii (lower left): The cliff face reaches a height of ~10 m and reveals large-scale foreset cross-beds (A2). Fig. Aiii (lower right): Solution tubes (S) are abundant in this exposure. B: Peppermint Grove. Fig. Bi (left): Shell-rich estuarine beds (E, OSL sample) capped by a palaeosol (P) and low-angled dune cross beds (A) adjacent to Scott's College boat shed and jetty. The estuarine beds appear to onlap older aeolianite (shown in Fig. Bii) – they sit within the channel cut into the older aeolianite by the Swan River. The bag is 0.5 m high. Fig. Bii (right): Thick (9 m) dune foreset beds (A, OSL sample taken from this unit ~40 m to W) and large solution tube (S) in an aeolianite exposure ~150 m N of Scott's College boat shed. C: Minim Cove. Fig. Ci (top): Composite image of shell-rich estuarine beds (E) exposed in the bank of the estuary, ~50 m E of Minim Cove jetty. A shell-rich bed (S) sits at the top of the section, ~4 m above the high tide mark. Fig. Cii (lower right): Estuarine beds (E) with scattered shells are capped by calcrete (C) and a palaeosol (P) with abundant rhizoliths (R), ~30 m E of jetty. The section is ~10 high. Aeolianite foreset beds (OSL sample) crop out above this exposure. Fig. Ciii (lower left): Shell-rich estuarine beds (OSL sample, arrow indicates visible shells) ~400 m E of jetty, that sit ~1.5 m above the high tide mark. D: North Fremantle. Dune topset beds (A, OSL sample) with abundant rhizoliths (R), exposed in a cutting in the aeolianite. E: Cottesloe Beach. This is the southern end of the shoreline exposure where the basal calcarenite (C) is onlapped by upward fining and seaward dipping beds of gravely beach sand (B, OSL sample). The beach deposits are unconformably overlain by dune foresets (A, OSL sample) with abundant solution tubes (S). Bioclastic gravelly beds are best exposed in an undercut intertidal section of cliff ~20 m further N (arrow). The section shown rises to ~6 m above MSL. F: Rottnest Island. Aeolianite at Bathurst Point, below the lighthouse (top right). The two thick dune units (A1 and A2, both sampled for OSL) are separated by a palaeosol (P).

estuarine beds is 177 ± 11/290 ± 29 ka (PG01). The previously reported ages for this unit, MIS 7 (Hewgill et al., 1983; Murray-Wallace and Kimber, 1989) and MIS 9 (Hearty, 2003) indicate that the older OSL age estimate is the most likely age for the estuarine deposits. Stratigraphically, the thick aeolianite unit is interpreted to sit below the estuarine beds (Fig. 3G), which suggests the older OSL age estimate for sample PG02 (415 ± 70 ka) is likewise the most likely age for this unit. The existence of the lower dose component

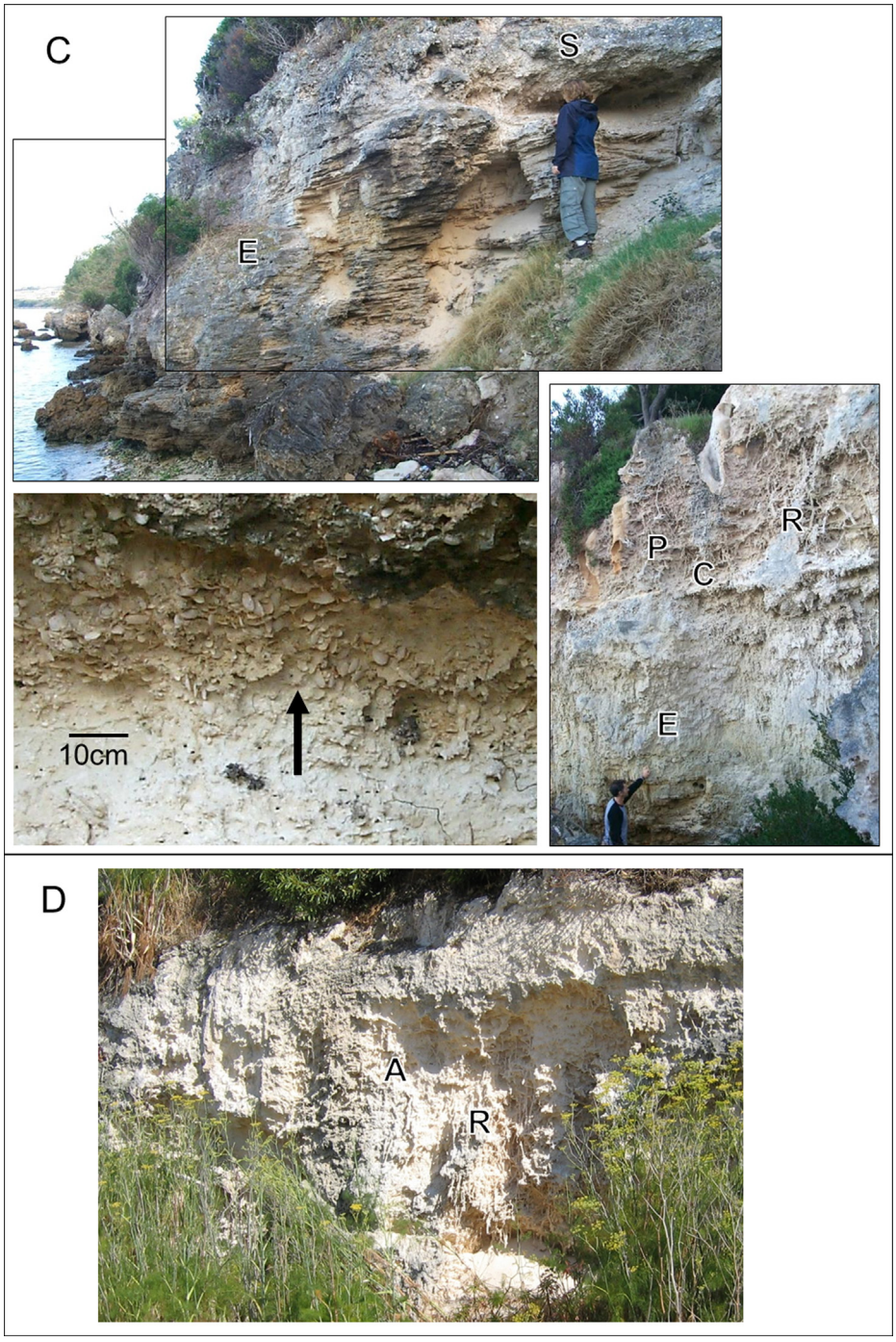

Fig. 4. (*continued*).

in each case requires further investigation, however, they possibly relate to contaminants introduced during sampling or preparation, or, are grains subject to a lower β dose rate due to, for example, being encased in thick $CaCO_3$ rinds. Regardless of the cause, the finite mixture model has successfully identified the upper dose component which is accepted as the burial dose for reasons of stratigraphy/corroborating chronology.

The basal unit at Minim Cove comprises horizontal to low-angle sandy shell-rich beds and beds of coarse to medium sand (Figs. 3C and 4C). The molluscan assemblage indicates a lower estuarine sand bank environment (Kendrick et al., 1991) of Last Interglacial age, MIS 5e (mollusc ESR ages, Hewgill et al., 1983; mollusc AAR ages, Murray-Wallace and Kimber, 1989). At the top of the estuarine deposit there is a weakly developed palaeosol, above which lie thick (up to 10 m) aeolianite cross-beds (Fig. 3C). Similar OSL ages were obtained for the estuarine beds (MC01, 108 ± 9 ka) and the overlying aeolianite (MC02, 115 ± 10 ka, Table 4) and show that both facies were emplaced during or shortly after the Last Interglacial, in the period represented by MIS 5e to 5b.

4.6. Cottesloe Beach

Beach and dune units at Cottesloe Beach are exposed in an intertidal platform and shoreline cliff cut into the Tamala

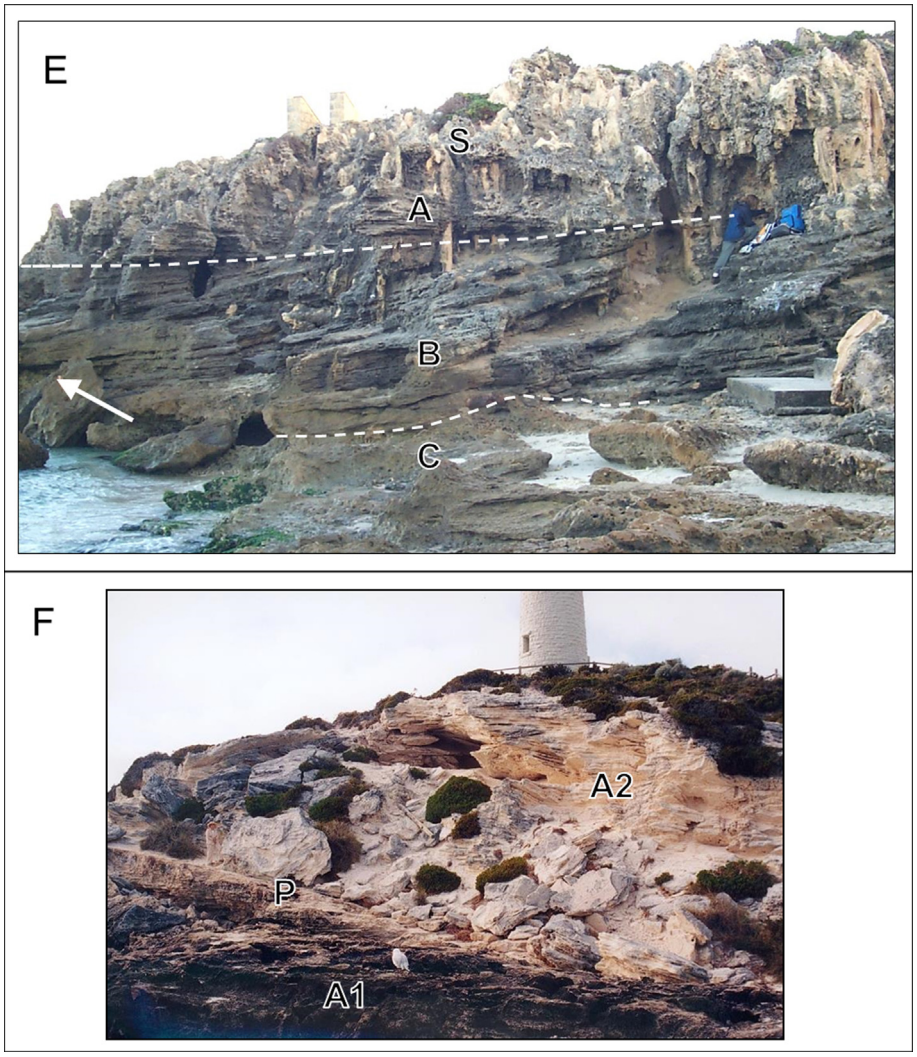

Fig. 4. (*continued*).

Limestone. The basal unit is heavily cemented calcarenite with no discernible bedding (Figs. 3E and 4E). A few *in-situ* fossil corals (undated) encrust the basal calcarenite, which is onlapped by beach gravel beds rich in coral and molluscan fragments (Fig. 3E). The gravel beds grade upward into coarse to medium sand, deposited as low-angle seaward dipping planar beds, a succession typical of a beach foreshore. In turn, the beach beds fine upwards and are then unconformably overlain by moderately to steeply landward-dipping dune foreset strata, emplaced under westerly (onshore) winds. The dune foresets attain a maximum thickness of 6 m, exhibit subaerial weathering features such as solution tubes and are capped by a well-developed reddish-brown palaeosol. In summary, the succession records marine erosion of the basal calcarenite, incipient coral growth, the accumulation of bioclastic gravel and sandy foreshore beds, the onset of aeolian deposition and a subsequent long period of subaerial weathering and soil formation. An AAR age estimate for the aeolianite is MIS 5e (Hearty, 2003), while TL ages for the aeolianite and beach deposit are 79 ± 9 and 78 ± 6 ka respectively (Price et al., 2001). The OSL age for the beach unit (CB02), 105 ± 9 ka, and the overlying aeolianite (CB01), 114 ± 9 ka, are significantly older than the TL ages (discussed in Section 5.1) and indicate deposition of both units during or shortly after the Last Interglacial.

4.7. Fremantle

The western margin of the aeolianite ridge was also sampled in a shoreline cliff near the Roundhouse (Fort) at Fremantle and in a cutting at North Fremantle (Figs. 3D and 4D). The shoreline section comprises dune foreset beds up to 8 m thick, with calcrete layers, solution pipes and a reddish palaeosol cap. The face of the cutting at North Fremantle comprises a thick set of low-angle cross beds, typical of a dune topset, with abundant rhizoliths and thin calcrete bands. An AAR age estimate for the Roundhouse aeolianite is middle Pleistocene (Hearty, 2003), while a TL age for this deposit is 72.4 ± 5 ka (Price et al., 2001). The exposure in the aeolianite cutting at North Fremantle has not previously been dated. OSL ages for the Roundhouse (RH01), 103 ± 10 ka, and North Fremantle (F01), 120 ± 12 ka, indicate both aeolianite units were deposited during or shortly after the Last Interglacial (age differences are discussed in Section 5.1).

4.8. Rottnest Island

Exposures examined at Bathurst Point comprise two thick aeolianite units separated by a palaeosol (Figs. 3F and 4F). The lower dune unit comprises foreset cross-beds with an easterly dip and is capped by a reddish-brown palaeosol and calcrete crust. The

Table 3
Radionuclide activities and dose rates for the OSL samples from Perth and Rottnest Island. All radionuclide values are in Bq kg^{-1}.

Sample	^{238}U	^{226}Ra	^{210}Pb	^{232}Th	^{40}K	Dose rate (Gy ka^{-1})
RI01	10.45 ± 0.84	4.61 ± 0.14	5.60 ± 0.98	2.16 ± 0.21	21.7 ± 1.6	0.30 ± 0.03
RI02	10.97 ± 0.69	9.28 ± 0.13	7.28 ± 0.82	3.64 ± 0.17	15.5 ± 1.2	0.32 ± 0.03
CB01	5.6 ± 0.8	6.5 ± 0.1	5.2 ± 0.9	6.2 ± 0.2	200 ± 3	0.89 ± 0.06
CB02	8.2 ± 1.0	6.6 ± 0.2	6.6 ± 1.1	5.9 ± 0.2	211 ± 3	0.99 ± 0.07
F01	8.2 ± 0.7	8.5 ± 0.1	7.9 ± 0.9	4.7 ± 0.2	120 ± 2	0.71 ± 0.05
RH01	10.7 ± 0.9	10.1 ± 0.2	10.1 ± 1.1	5.4 ± 0.2	133 ± 3	0.80 ± 0.06
MC01	9.5 ± 0.8	8.8 ± 0.1	8.8 ± 0.8	3.5 ± 0.2	156 ± 3	0.80 ± 0.06
MC02	12.7 ± 0.8	13.0 ± 0.2	12.4 ± 0.9	5.7 ± 0.3	226 ± 3	1.00 ± 0.08
PG01	5.1 ± 1.3	6.8 ± 0.2	7.7 ± 1.6	14.1 ± 0.3	270 ± 5	1.26 ± 0.09
PG02	8.2 ± 0.9	9.1 ± 0.2	8.7 ± 1.0	6.6 ± 0.2	174 ± 3	0.89 ± 0.07
KP01	6.5 ± 0.8	6.3 ± 0.1	5.7 ± 1.0	11.9 ± 0.3	181 ± 3	0.91 ± 0.07
KP02	3.35 ± 0.54	3.78 ± 0.08	4.99 ± 0.71	5.24 ± 0.10	164 ± 2	0.79 ± 0.04

palaeosol represents a major late Pleistocene hiatus in sediment accumulation on Rottnest Island (Hearty, 2003). The upper unit comprises thick foreset beds with an easterly dip, and forms the majority of the island's land mass (Hearty, 2003). A TL age for the lower dune unit is 67 ± 9 ka and the upper dune is 20 ± 2 ka (samples W2370 and W2371 in Price et al., 2001). From this study, the lower dune unit at Bathurst Point has an OSL age of 77 ± 12 ka (RI01, Table 4) which spans the period represented by MIS 5a to MIS 4. The OSL age of the upper aeolianite, 27.0 ± 4.5 ka (RI02), indicates deposition during the period from late MIS 3 to early MIS 2. In contrast, based on whole-rock AAR analyses, the lower dune unit was assigned an age that falls within the period represented by MIS 5e (132–118 ka) and the upper unit the period from MIS 5c–5a, approximately 110–75 ka (Hearty, 2003).

5. Discussion

5.1. Chronological data

The ages that are available for the aeolianite examined around Perth, derived from a number of dating methods, show varying levels of agreement. Previously reported TL ages for dune and beach units in the aeolianite around Perth and on Rottnest Island are consistently younger than OSL ages for these units (apart from the Kings Park sample KP01). However, in most cases the ages overlap within their two sigma uncertainties (double the one sigma age uncertainties shown in Tables 2 and 4). The estuarine beds at Minim Cove (MC02, OSL age: 104 ± 9 ka) and the beach unit at Cottesloe Beach (CB02, OSL age: 105 ± 9 ka) have OSL ages that are slightly younger than their previously reported AAR and ESR age estimates, MIS 5e (Table 2). Although these OSL ages are consistent stratigraphically, the shallow-marine deposits at Minim Cove and Cottesloe Beach rise at least 2 m above present mean sea level (Fig. 3C, E) and therefore very likely were deposited during the sea-level highstand of the Last Interglacial (Chappell et al., 1996) given the stability of the Perth coast over this period (Kendrick et al., 1991; Stirling et al., 1995, 1998). The OSL ages therefore appear too young. However, the two sigma uncertainties of the OSL ages (MC02 104 ± 18 ka; CB02, 105 ± 18 ka) overlap with the timing of the Last Interglacial highstand on this coast (128–116 ka, Stirling et al., 1998). Nathan and Mauz (2008) have shown that the infilling of interstitial pore space with secondary carbonates during the

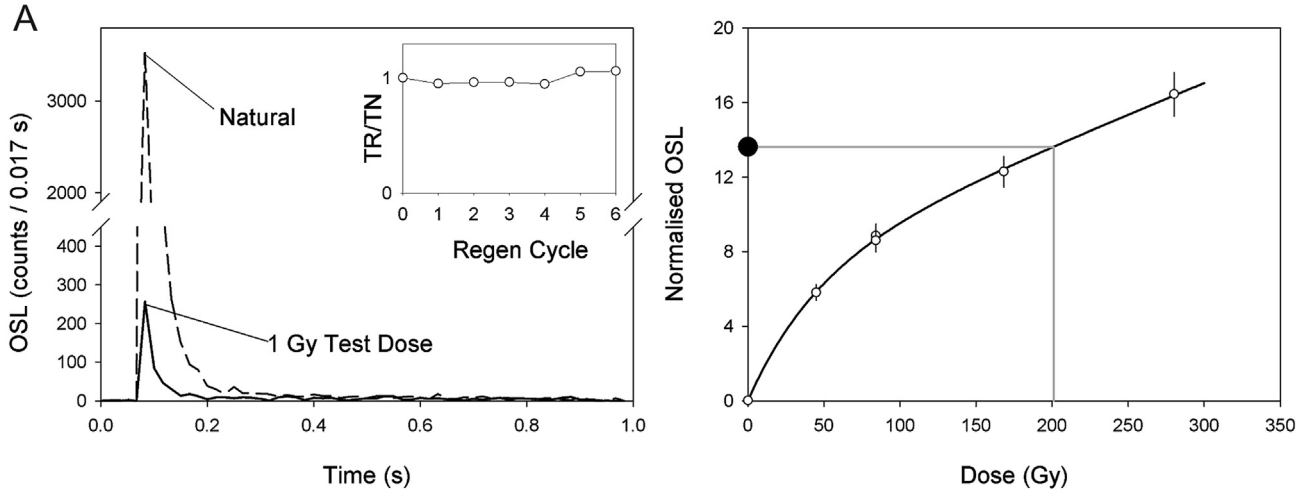

Fig. 5. Graphs of the OSL laboratory data. A: An example of data for a typical grain that was accepted as a reliable dosimeter. The left plot shows shine–down curves for the Natural Dose (broken line) and 1st Test Dose (solid line) for a single grain from sample KP01. Note the high sensitivity and rapid signal depletion to background. The inset shows the minimal change in test dose OSL (TR) throughout the analysis cycle. Note TR is normalised against the OSL of the first Test Dose, i.e. that following the Natural (TN). The right plot shows the sensitivity corrected OSL responses to the Natural Dose (Black circle) and the Regenerative Doses (White Circles), with the fitted growth curve (Black line) and the derived Natural Dose (Grey line). Note the zero growth-curve intercept, overlapping repeat points (at ~80 Gy), low uncertainties on the points and non-saturating Growth curve; which together indicate the suitability of this grain as a reliable dosimeter. B: Radial plots of the equivalent doses measured on single grains for the 12 samples. The measured D_e (in Gy) for a grain can be read by tracing a line from the *y*-axis origin through the point until the line intersects the radial axis (log scale) on the right-hand side. The corresponding standard error for this estimate can be read by extending a line vertically to intersect the *x*-axis. The *x*-axis has two scales: one plots the relative standard error of the D_e estimate (in %) and the other ('Precision') plots the reciprocal standard error. Values with the highest precisions and the smallest relative errors plot closest to the radial axis on the right of the diagram, and the least precise estimates plot furthest to the left. The shaded bands encompass those grains within 2sigma of the burial dose (grey line). For samples PG01 and PG02 the additional open bands are centred on the second dose component determined using the finite mixture model. For samples RI01 and RI02 a contamination signal is evident as a small proportion of grains centred on zero. These are assumed to have become admixed to the sample during initial sampling (most likely) or subsequent laboratory processing.

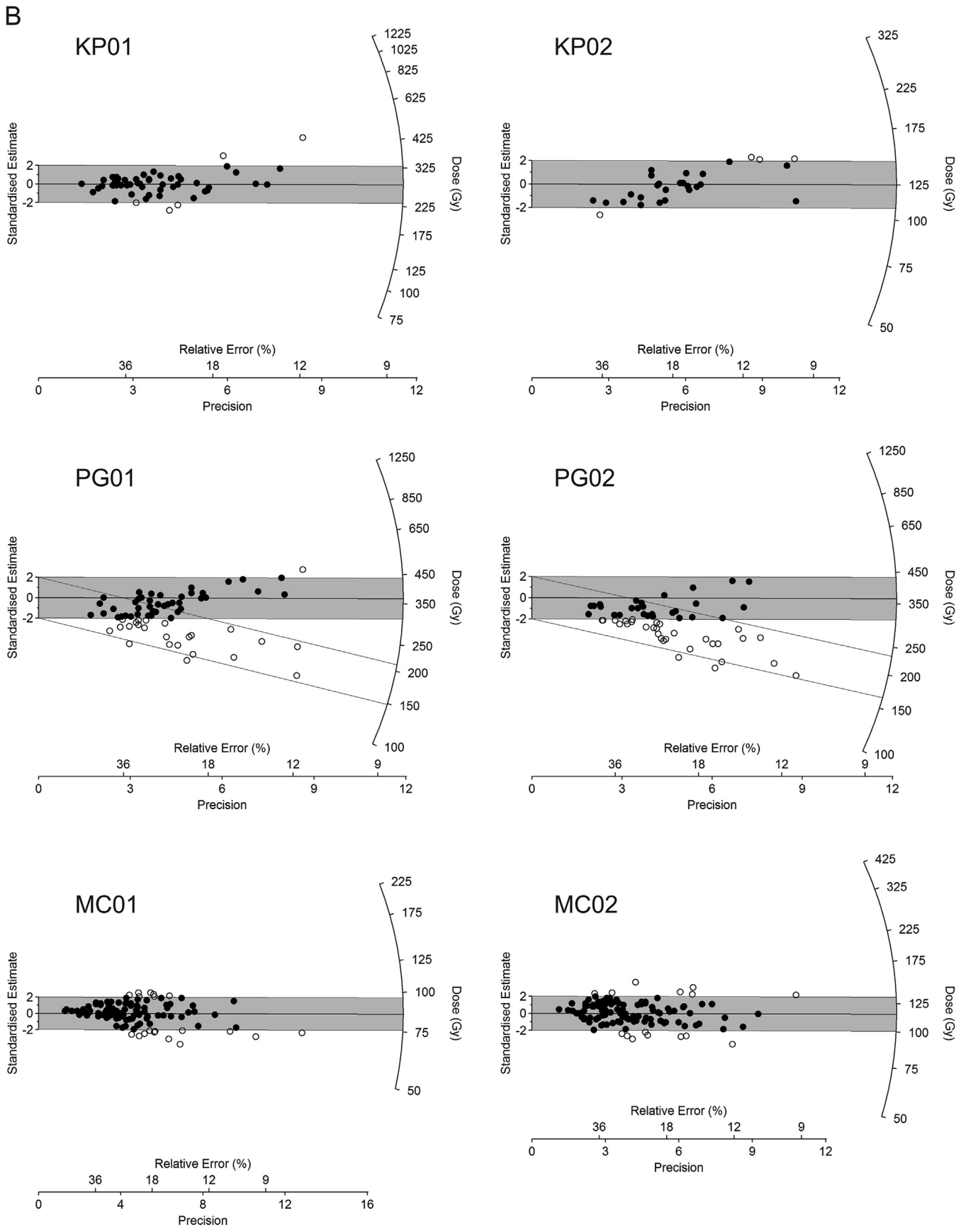

Fig. 5. (*continued*).

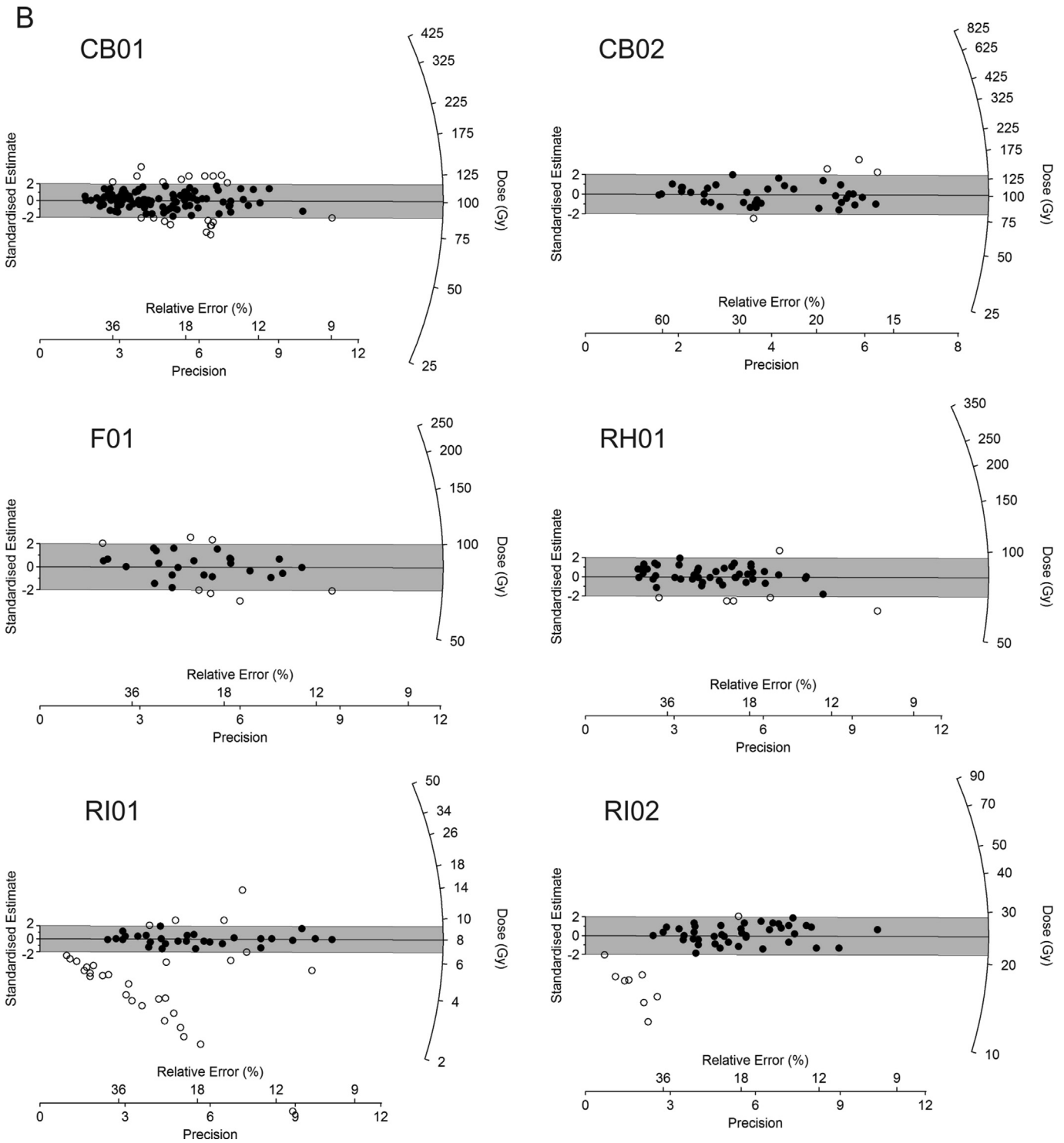

Fig. 5. (*continued*).

burial period could result in age underestimation for carbonate-rich sediments, and this may be a factor with these samples. They modelled age under-estimations of between 2 and 15% for samples where there has been a dramatic increase in carbonate content through the burial period. We consider it likely however, that for the samples analysed in this study the age under-estimation, if any, would be towards the lower end of this range. Significant effort went into selecting sample sites that were the best preserved/least altered parts of outcrops and the carbonate content appears to have changed little to moderately over time. A detailed petrological study of each sample would be required to more accurately/quantitatively assess how much carbonate may have been lost or gained over time, an exercise beyond the scope of the current work.

A further contributor to uncertainty on the OSL ages, for samples KP01 and RI02 at least, is the effect of variations in overburden thickness through the burial period on cosmic dose rate. These two

Table 4
OSL age data, including the measured equivalent dose (D_e), over-dispersion parameter (σd) and OSL age.

Sample	D_e (Gy)	σd (%)	Age (ka)
RI01	8 ± 1	18	27.0 ± 4.5
RI02	25 ± 3	5	77 ± 12
CB01	102 ± 3	22	114 ± 9
CB02	104 ± 5	18	105 ± 9
F01	85 ± 5	20	120 ± 12
RH01	83 ± 3	15	103 ± 10
MC01	86 ± 3	19	108 ± 9
MC02	116 ± 4	21	115 ± 10
PG01	177 ± 11 or 370 ± 23	15[a]	140 ± 14 or 290 ± 29
PG02	197 ± 10 or 370 ± 55	15[a]	220 ± 20 or 415 ± 70
KP01	280 ± 13	19	310 ± 30
KP02	125 ± 15	18	155 ± 20

[a] Assumed over-dispersion of modelled dose components within finite mixture model.

samples have evidence in their overlying profiles of depositional hiatuses in the form of palaeosol horizons, indicating that the sampling locations may have sat close (~6 m and ~4 m respectively) to the surface for a considerable proportion of the burial period. Modelling of this effect has shown, however, that even in a worse-case scenario, where the period spent close to the surface is set to equal the difference between the two ages calculated in these profiles, the age underestimation is less than half the uncertainty already provided. Accordingly, we have retained the as-calculated ages for these samples, in recognition that we cannot rule out that the soil horizon observed may have itself been buried for some of the period spanned by the two calculated ages. For the remaining samples, we have no reason to consider the long term burial depth to be very different from the observed burial depth, with the Cottesloe Beach location showing clearly that essentially single age units can be many metres thick.

The new OSL ages presented here represent a reliable preliminary chronological framework for the Tamala Limestone in the Perth region, which is likely representative of the extensive aeolianite coast and carbonate shelf south and north of Perth (Mayer, 2008; Playford et al., 2013). It is important to note, however, that replicate OSL dating of a single stratigraphic unit, with several sample sites and samples per unit, would likely significantly reduce the uncertainty in the representativeness of the single OSL ages obtained in this study in terms of the timing of major depositional phases, following the lead provided by Bateman et al. (2011) in their chronostratigraphic analysis of the coastal aeolianite and dunes of the Cape region of South Africa.

There are more significant discrepancies between the OSL and TL ages for the basal unit at Kings Park (KP01, Tables 2 and 4); and between the OSL/TL and AAR age estimates for Fremantle and Rottnest Island, where the AAR age estimates are consistently older. A detailed discussion of these dating methods is beyond the scope of this paper, however, we propose that the OSL method employed in this study has provided the most reliable estimates of the depositional age of the aeolianite (see Jacobs, 2008 for a comprehensive review of optical dating of coastal and marine sediments). The discrepancies between the OSL and TL ages likely reflect the use of single grain techniques in the former and large aliquot techniques (i.e. summing the light emitted from many thousands of grains at a time) for the latter. For the OSL techniques described here, on a grain by grain basis, relatively few grains could be shown to be reliable dosimeters. While 45–55% of grains produced measurable OSL signals, only ~9% of grains produced acceptable growth curves from which we could reliably determine a D_e. Large aliquot techniques (whether using TL or OSL) necessarily include contributions from these aberrant grains in every luminescence measurement, hence may be prone to either underestimation or overestimation in situations where the proportion of the light sum produced by these grains is high, in comparison to that produced by the grains shown to be reliable dosimeters. This is one possible explanation, however, we stress that we have not undertaken the in-depth investigations of the TL properties of these samples to attribute a cause definitively.

The discordances in OSL and AAR whole-rock ages are possibly due to differences between the age of the biogenic carbonate grains that are analysed in the AAR method and the depositional age of the dunes as indicated by the OSL ages of the quartz grains. The skeletal carbonate grains measured in the AAR whole-rock method may include a large proportion of relict grains reworked from older coastal or shelf deposits (discussed below). Therefore, the AAR ages may reflect the time of death of the fossil marine invertebrates from which the relict skeletal grains are derived, rather than the time that the aeolianite was deposited.

To provide age estimates for aeolianite on Rottnest Island that was deposited after MIS 5e, the AAR whole-rock data for Rottnest Island were correlated by Hearty (2003) with the calculated ages derived from similar AAR data for late Pleistocene aeolianite on Bermuda. This approach appears problematic because the mode of aeolianite formation on Bermuda, where the 'highstand aeolianite model' has been developed (Hearty and O'Leary, 2008), varies significantly from Rottnest Island. The Bermuda islands have fundamentally different shelf sediment systems – the shallow depth (~20 m) of the shelf appears to limit carbonate sediment production to periods of high or relatively high sea level (e.g. MIS 5e, 5c, 5a; Vacher et al., 1995). In contrast, the extensive Rottnest Shelf grades gently offshore to depths of around 75 m before there is any significant break in slope (Brooke et al., 2010; Fig. 2), indicating the high potential for carbonate production and movement onshore into dunes throughout much of the glacial–interglacial cycle, at least during the extensive periods when sea level is at or above this depth (Siddall et al., 2006).

5.2. Aeolianite landforms

The Perth aeolianite ridge sampled is clearly a composite structure (Fig. 3G). At Kings Park, the most landward (eastern) component of the ridge comprises dunes deposited at 310 ± 30 ka (KP01) and 155 ± 20 ka (KP02, Table 4). The palaeosol that caps the lower unit, therefore, potentially represents a period of subaerial exposure of up to 150,000 years. The lower dune unit may have been sourced from a nearby interglacial shoreline while the upper unit was likely reworked from a relict coastal deposit during the MIS 6 glacial period (Fig. 6), when the shoreline was located more than 40 km to the west. The seaward margin of the ridge, in contrast, comprises dunes that were emplaced during the middle Pleistocene and subsequently onlapped by younger middle Pleistocene estuarine sediments (Peppermint Grove, Fig. 3G), as well as Last Interglacial estuarine (Minim Cove) and beach beds (Cottesloe), and finally dunes were deposited during and shortly after the Last Interglacial (Minim Cove, Cottesloe, Fremantle, Fig. 3G). This stacking and partial erosion of barrier deposits is a function of the tectonic stability of the coast and the underlying gradient of the surface on which the Pleistocene barrier deposits sit. For example, Brooke et al. (2010) record the increase in elevation of the base of the three discernible onshore aeoliante ridges with distance inland from the Perth coast. The stability and coastal gradient likely restricts the accommodation space available for barrier deposition during highstands, resulting in the stacking of deposits (Roy et al., 1994; Bateman et al., 2011).

The broad-scale morphology of the extensive aeolianite ridge complex on the Swan Coastal Plain has been partly shaped by

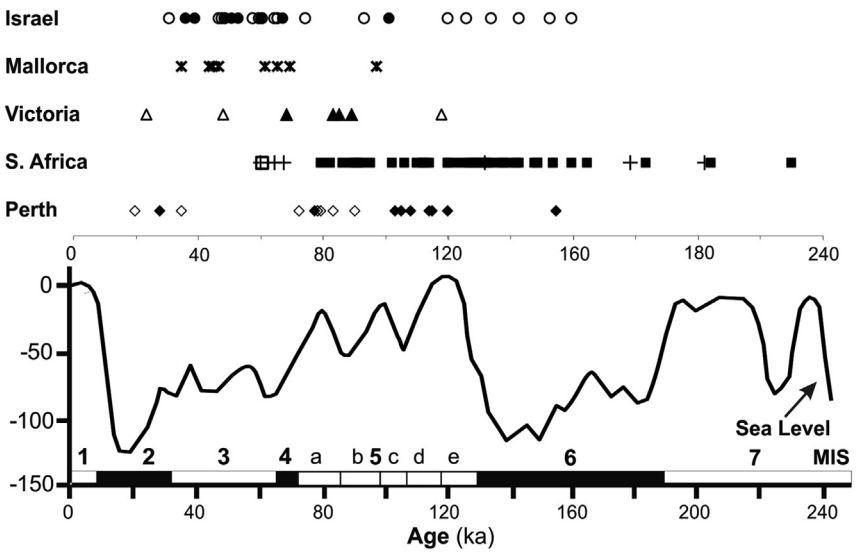

Fig. 6. A plot of optical ages of aeolianite (without error bars for clarity) on the margins of stable, low-gradient carbonate continental shelves and a sea level curve for the last two glacial–interglacial cycles (after Siddall et al., 2006). The black diamonds are the new OSL ages for Perth (excluding the older OSL ages for Peppermint Grove, 290 ± 29 ka, 415 ± 70 ka, and Kings Park, 320 ± 30 ka); the open diamonds are previously published TL ages for Perth (Price et al., 2001). Data for South Africa: OSL ages (black squares) from Bateman et al. (2011); IRSL ages (crosses) from Porat and Botha (2008); IRSL age (open square) from Cawthra et al. (2012). Victoria (SE Australia): Gardner et al. (2006) (black triangles) and Zhou et al. (1994) (open triangles). Mallorca: Fornos et al., 2009. Israel: Frechen et al., 2004 (open circles), Sivan and Porat, 2004 (black circles). The marine isotope stages are from Imbrie et al. (1984).

shoreline erosion of older deposits during sea-level highstands – the modern shoreline at Cottesloe, where wave erosion has exposed MIS 5 dune and beach units and the underlying middle Pleistocene calcarenite, shows that significant coastal erosion occurs during interglacials (e.g., Fig. 2; Gozzard, 2007). Reworking of deposits during glacial periods likewise modifies the original coastal dune morphology. Luminescence ages of extensive Pleistocene aeolianite ridges on the coastal plain of Israel (Sivan and Porat, 2004) and aeolianite barrier deposits in South Africa (Porat and Botha, 2008; Bateman et al., 2011) likewise reveal the composite structure of these coastal landforms (Fig. 6). The barriers of the Coorong Coastal Plain are also composite features (e.g. Woakwine I and II; Robe I, II and III, Murray-Wallace, 2002).

5.3. Glacial-age deposits

The OSL and TL ages for Rottnest Island record major phases of dune accumulation well after deposition of the island's basal calcarenite and Last Interglacial coral reef (Stirling et al., 1998). Optical ages of the lower dune unit at Bathurst Point (OSL, RI01, 77 ± 12 ka; TL 67 ± 12 ka) record a major phase of dune deposition during the period from MIS 5a to MIS 4, when sea level ranged between 20 and 70 m below the present level (Siddall et al., 2006). Relict dune landforms on the outer shelf in this region appear to have been sourced from a shoreline that sat around 50–60 m below present sea level. The DEM for this area reveals a connection between the western margin of Rottnest Island and this palaeoshoreline (Fig. 2C; Brooke et al., 2010; Nicholas et al., 2013). The DEM also reveals the connection between the island and the recurved palaeoshoreline on the inner shelf southeast of the island (Fig. 2A). Based on these morphological data, the OSL and TL ages for the island and TL ages for Point Peron and Penguin Is (Table 2), it seems likely that a large proportion of the aeolianite on Rottnest Island comprises carbonate sand that was originally derived from biogenic production on the shelf between the period from MIS 5a to 3, when sea level was around 70–30 m lower than present and the middle and outer Rottnest Shelf formed a shallow sea (Figs. 2A and 6). Although sea surface temperatures were a few degrees lower than present during this period, the Leeuwin current was active (McCulloch and Esat, 2000; Wyrwoll et al., 2009; Spooner et al., 2011; Petherick et al., 2013) and heterozoan biota on the shelf produced abundant carbonate sediment. For example, shelf deposits of MIS 3 age occur extensively along the shelf of southern Australia (Rivers et al., 2007).

The optical ages for the upper dune unit at Bathurst Point (OSL, RI02, 27.0 ± 4.5 ka; TL 19 ± 3 ka) are consistent with deposition shortly before or during the Last Glacial Maximum. At this time, dune sediment would have been sourced from stranded shelf deposits, such as those generated when the shoreline sat around 60 m below present, rather than the LGM shoreline which was located on the relatively steep outer margin of the continental shelf some 17 km to the west (Brooke et al., 2010; Fig. 2B). Aeolianite deposited during the period from MIS4 to MIS 2 has also been reported on the Channel Islands off the coast of southern California (Johnson, 1977; Muhs, 1992; Muhs et al., 2009), on the coast of South Africa (Bateman et al., 2004, 2011; Porat and Botha, 2008), Mallorca (Fornos et al., 2009) and Victoria in southeastern Australia (Zhou et al., 1994; Gardner et al., 2006), and on the inner shelf off the eastern coast of South Africa (Cawthra et al., 2012; Fig. 6).

During the Last Glacial Maximum the western region of Australia experienced a decrease in rainfall and strong prevailing southerly and westerly winds (Shulmiester et al., 2004; Playford et al., 2013). These conditions likely produced lower rates of cementation in exposed marine carbonate sands and coastal dunes (e.g. Kindler and Mazzolini, 2001). During the LGM, therefore, there was a greater potential for unlithified carbonate shelf and coastal sediment of MIS 3 age and older (e.g. MIS 5a) to be reworked by wind into mobile dunes. For example, relict dune structures on the continental shelf south of Rottnest Island and central Western Australia extended up to 15 km across the now drowned shelf (Brooke et al., 2010; Nichol and Brooke, 2011). The Last Interglacial coral reef and calcarenite of Rottnest Island (Stirling et al., 1995; Price et al., 2001), and deposits emplaced during periods of intermediate sea level (e.g. MIS 3 to 5a, Table 2), apparently formed an anchor point for relict shelf sediment that was reworked into these mobile dunes during the Last Glacial. Rottnest Island, therefore,

provides an important record of aeolianite formation over a wide range of sea levels and climatic conditions that contrast with aeolianite records from oceanic islands such as Bermuda and the Bahamas (Fig. 3G).

5.4. Continental shelf sedimentation

Remnant barriers and dune fields on the Rottnest Shelf record past major phases of sediment accumulation and mobilization (Fig. 2A). Notwithstanding the potential underestimation of the TL ages (Section 5.1), it is worth noting that TL ages for aeolianite on Penguin Island and Point Peron (78 ± 5 ka and 90 ± 4 ka respectively; Price et al., 2001; Table 2) are similar to the OSL age of the basal aeolianite at Bathurst Point (77 ± 12 ka, RI02; Fig. 4). These deposits and Five Fathom Bank are remnants of an aeolianite coast that extended from Point Peron to Rottnest Island (Figs. 1 and 2), when sea level was 30–20 m below present (Fig. 2; Playford, 1988; Brooke et al., 2010), as occurred in MIS 5c and 5a (Chappell et al., 1996).

The extensive ridge feature on the outer Rottnest Shelf that rises from depths of 60 to 50 m, is also likely the remnant of a barrier that formed when sea level was significantly lower than present (Fig. 2B; Brooke et al., 2010; Nicholas et al., 2013). The morphology and basal depth of this outer shelf feature indicates one or more shorelines formed here during MIS 3/4 (Fig. 2). Although there are no age data available for the submerged components of these shelf structures to test this interpretation, there was likely a high potential for sediment delivery to shorelines at these times of intermediate sea level – the shallow-water setting formed on the shelf at these times likely enhanced carbonate production and/or its transport onshore into beach and ultimately coastal dune deposits (e.g. Vacher and Rowe, 1997; Brooke et al., 2003).

Extensive linear submerged features have been reported at similar depths on carbonate continental shelves off the aeolianite coasts of central Western Australia (Nichol and Brooke, 2011), southeastern Australia (Sprigg, 1979), southern and eastern South Africa (Birch et al., 1978; Martin and Flemming, 1986; Bateman et al., 2004, 2011; Cawthra et al., 2012) and Mozambique (Ramsay, 1994). These features appear to be remnants of coastal barriers that have likewise at least partially withstood erosion during the post-glacial marine transgression and the Holocene highstand. They record the formation of extensive coastal dunes on areas of subaerially exposed continental shelf. Based on these records and the Perth region data (Fig. 6), a conceptual model of Quaternary continental shelf carbonate deposition and aeolianite landform evolution on stable continental margins is proposed (Fig. 7). The model relates the position, morphology and age of these types of large-scale coastal deposits to major phases of production, deposition, erosion and reworking of carbonate sediment that occur at various stands of the sea during a Quaternary glacial–interglacial cycle.

A key element of this model (Fig. 7) is the formation of shoreline barriers and coastal dunes during a wide range of sea-level positions, during glacial and interglacial periods. In particular, the model depicts the formation of these deposits on continental shelves that slope gently to the outer margin of the shelf, down to depths significantly greater than is common on shelves that typically surround oceanic aeolianite islands (e.g. Bermuda ~20 m; Bahamas

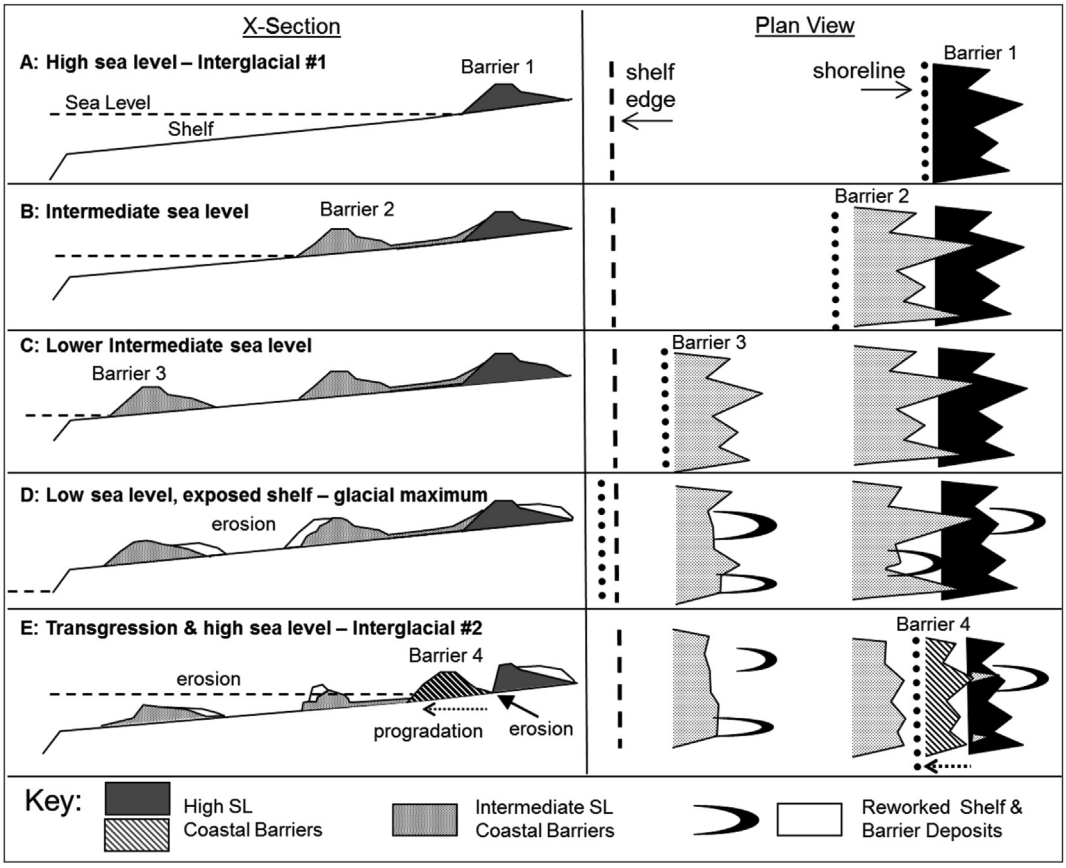

Fig. 7. A conceptual model of the cycle of middle–late Quaternary carbonate sedimentation and coastal aeolianite landform evolution that occurs on stable continental shelves (discussed in Section 5.4), based on the Perth region data and the studies referred to in Fig. 6.

~25 m). These islands are typically rimmed by shallow shelves that drop off steeply into much deeper water (100 s–1000 s of m). As a consequence, the majority of carbonate sediments around oceanic islands are produced during periods of high and relatively high sea level, while in continental shelf settings aeolianite formation can occur during periods of much lower sea level, potentially over the full range of a Quaternary glacial–interglacial sea level cycle. Additionally, continental margins commonly experience arid conditions during glacial periods that enhance the potential for the reactivation of coastal deposits. The model describes the reoccurrence of these long-term shelf processes and their cumulative geomorphic imprint on continental shelves and coasts (Fig. 7).

6. Conclusions

The optical ages, stratigraphy and morphology of aeolianite around Perth and drowned coastal landforms on the adjacent Rottnest Shelf, Western Australia, are similar to coastal aeolianite and shelf structures that occur on a range of low-gradient carbonate continental shelves in both hemispheres. These data indicate that coastal carbonate barriers and dune fields form under a wide range of climatic conditions and sea levels. In addition to many well-preserved examples of barriers that were largely formed during the Last Interglacial (MIS 5e), barriers have also developed on continental shelves during periods when sea level was around 20 and 60 m lower than present. Shelves that grade gently to greater depths have the potential to have had carbonate shoreline deposits emplaced over the full depth range (~125 m) of the Quaternary sea-level cycle. During the Last Glacial Maximum, exposed shelf sediment and stranded coastal barriers on the Rottnest Shelf were partly reworked into mobile dunes, indicating how aeolianite landforms and islands on continental margins can include units emplaced during sea-level lowstands.

On continental shelves, large-scale, broadly shore-parallel coastal aeolianite ridges are commonly complex structures, built of sediment sourced from shallow-water and shoreline environments that formed under high and intermediate sea levels. The morphology of many of these deposits has been partly shaped by shoreline erosion during highstands as well as reworking during glacial periods, rather than representing the original depositional morphology of the barrier. Given the high potential for reworking of this shelf and coastal sediment prior to its final deposition and cementation, OSL is an effective method for dating these deposits.

Acknowledgements

Thanks to Lynda Radke, Darren Skene and Claire Taylor for assistance in the field, and Tanya Whiteway, Kim Picard and Olivia Wilson for elevation data mapping. Scott Nichol, Dan Muhs and an anonymous reviewer provided insightful reviews that significantly improved the paper. PP and PH publish with the permission of the Director of the Geological Survey of Western Australia, and BB with permission of the Chief Executive Officer of Geoscience Australia.

References

Aitken, M.J., 1998. An Introduction to Optical Dating. The Dating of Quaternary Sediments by the Use of Photon-stimulated Luminescence. Oxford University Press, Oxford, p. 267.

Bateman, M.D., Carr, A.S., Dunajko, A.C., Holmes, P.J., Roberts, D.L., McLaren, S.J., Bryant, R.G., Marker, M.E., Murray-Wallace, C.V., 2011. The evolution of coastal barrier systems: a case study of the Middle–Late Pleistocene Wilderness barriers, South Africa. Quat. Sci. Rev. 30, 63–81.

Bateman, M.D., Holmes, P.J., Carr, A.S., Horton, B.P., Jaiswal, M.K., 2004. Aeolianite and barrier dune construction spanning the last two glacial–interglacial cycles from the southern Cape coast, South Africa. Quat. Sci. Rev. 23, 1681–1698.

Birch, G.F., De Plessis, A., Willis, J.P., 1978. Off shore and on land geological and geophysical investigations in the Wilderness Lakes region. Trans. Geol. Soc. S. Afr. 81, 339–352.

Botter-Jensen, L., Bulur, E., Duller, G.A.T., Murray, A.S., 2000. Advances in luminescence instrument systems. Radiat. Meas. 32, 523–528.

Brooke, B., 2001. The distribution of carbonate eolianite. Earth Sci. Rev. 55, 135–164.

Brooke, B., Creasey, J., Sexton, M., 2010. Broad-scale geomorphology and benthic habitats of the Perth coastal plain and Rottnest Shelf, Western Australia, identified in a merged topographic and bathymetric digital relief model. Int. J. Remote Sens. 31, 6223–6237.

Brooke, B.P., Woodroffe, C.D., Murray-Wallace, C.V., Heijnis, H.R., 2003. Quaternary calcarenite stratigraphy on Lord Howe Island, south-western Pacific Ocean and the record of coastal carbonate deposition. Quat. Sci. Rev. 22, 859–880.

Bureau of Meteorology, 2012. Summary Statistics for Perth Metro. http://www.bom.gov.au/climate/averages/tables/cw_009225.shtml.

Cawthra, H.C., Uken, R., Ovechkina, M.N., 2012. New insights into the geological evolution of the Durban Bluff and adjacent Blood Reef, South Africa. S. Afr. J. Geol. 115, 291–308.

Carew, J.L., Mylroie, J.E., 1997. Geology of the Bahamas. In: Vacher, H.L., Quinn, T.M. (Eds.), Geology and Hydrogeology of Carbonate Islands, Developments in Sedimentology, vol. 54. Elsevier, H. L. Amsterdam, pp. 91–139.

Carr, A.S., Bateman, M.D., Holmes, P.J., 2007. Developing a 150 ka luminescence chronology for the coastal dunes of the southern Cape, South Africa. Quat. Geochronol. 2, 110–116.

Chappell, J., Omura, A., Esat, T., McCulloch, M., Pandolfi, J., Ota, Y., Pillans, B., 1996. Reconciliation of late Quaternary sea levels derived from coral terraces at Huon Peninsula with deep sea oxygen isotope records. Earth Planet. Sci. Lett. 141, 227–236.

Collins, L.B., 1988. Sediments and history of the Rottnest Shelf, southwest Australia: a swell-dominated, non-tropical carbonate margin. Sediment. Geol. 60, 15–49.

Fairbridge, R.W., Teichert, C., 1953. Soil horizons and marine bands in the coastal limestones of Western Australia. Proc. R. Soc. N. S. W. 86, 68–87.

Fornos, J.J., Clemmensen, L.B., Gomez-Pujol, B.L., Murray, A.S., 2009. Late Pleistocene carbonate aeolianites on Mallorca, Western Mediterranean: a luminescence chronology. Quat. Sci. Rev. 28, 2697–2709.

Frechen, M., Neberb, A., Tsatskinc, A., Boenigkc, W., Ronenc, A., 2004. Chronology of Pleistocene sedimentary cycles in the Carmel Coastal Plain of Israel. Quat. Int. 121, 41–52.

Galbraith, R.F., 2005. Statistics for Fission Track Analysis. Chapman & Hall/CRC Press, Boca Raton.

Galbraith, R.F., Roberts, R.G., Laslett, G.M., Yoshida, H., Olley, J.M., 1999. Optical dating of single and multiple grains of quartz from Jinmium rock shelter, northern Australia: Part I, experimental design and statistical models. Archaeometry 41, 339–364.

Gardner, T.W., Webb, J., Davis, A.G., Cassel, E.J., Pezzia, C., Merritts, D.J., Smith, B., 2006. Late Pleistocene landscape response to climate change: eolian and alluvial fan deposition, Cape Liptrap, southeastern Australia. Quat. Sci. Rev. 25, 1552–1569.

Gozzard, J.R., 2007. Geology and Landforms of the Perth Region. Geological Survey of Western Australia, Perth.

Hearty, P.J., 2003. Stratigraphy and timing of eolianite deposition on Rottnest Island, Western Australia. Quat. Res. 60, 211–222.

Hearty, P.J., O'Leary, M.J., 2008. Carbonate eolianites, quartz sands, and Quaternary sea-level cycles, Western Australia: a chronostratigraphic approach. Quat. Geochronol. 3, 26–55.

Hewgill, F.R., Kendrick, G.W., Webb, R.J., Wyrwoll, K.-H., 1983. Routine ESR dating of emergent Pleistocene marine units in Western Australia. Search 14, 215–217.

Imbrie, J., Hays, J.D., Martinson, D.G., McIntyre, A., Mix, A.C., Morley, J.J., Pisias, N.G., Prell, W.L., Shackelton, N.J., 1984. The orbital theory of Pleistocene climate: support from a revised chronology of the marine ^{18}O record. In: Berger, A.L., Imbrie, J., Hays, J., Kukla, G., Saltzman, B. (Eds.), Milankovitch and Climate, Understanding the Response to Astronomical Forcing. Reidel, Dordrecht, pp. 269–305.

Jacobs, Z., 2008. Luminescence chronologies for coastal and marine sediments. Boreas 37, 508–535.

James, N.P., Collins, L.B., Bone, Y., Hallock, P., 1999. Carbonates in a temperate realm: modern sediments on the southwest Australian shelf. J. Sediment. Res. 69, 1297–1321.

Johnson, D.L., 1977. The late Quaternary climate of coastal California: evidence for an Ice Age refugium. Quat. Res. 8, 154–179.

Kelletat, D., 1991. Geomorphological aspects of eolianites in Western Australia. In: Bruckner, H., Radtke, U. (Eds.), Von der Nordsee bis zum Inischen Ozsean. Franz Steiner Verlag, Stuttgart, pp. 181–198.

Kendrick, G.W., Wyrwoll, K.-H., Szabo, B.J., 1991. Pliocene–Pleistocene coastal events and history along the western margin of Australia. Quat. Sci. Rev. 10, 419–439.

Kindler, P., Hearty, P.J., 1997. Geology of the Bahamas: architecture of Bahamian Islands. In: Vacher, H.L., Quinn, T.M. (Eds.), Geology and Hydrogeology of Carbonate Islands, Developments in Sedimentology, vol. 54. Elsevier, H. L. Amsterdam, pp. 141–160.

Kindler, P., Mazzolini, D., 2001. Sedimentology and petrography of dredged carbonate sands from Stocking Island (Bahamas). Implications for meteoric diagenesis and aeolianite formation. Palaeogeogr. Palaeoclimatol. Palaeoecol. 175, 369–379.

Martin, A.K., Flemming, B.W., 1986. The Holocene shelf sediment wedge off the south and east coast of South Africa. In: Knight, R.J., McLean, J.R. (Eds.), Shelf Sands and Sandstones, Memoir II. Canadian Society of Petroleum Geologists, pp. 27–44.
Mayer, W., 2008. Early geological investigations of the Pleistocene Tamala Limestone, Western Australia. In: Grapes, R.H., Oldroyd, D., Grigelis, A. (Eds.), History of Geomorphology and Quaternary Geology, Geological Society, London, Special Publications 301, pp. 279–293.
McCulloch, M.T., Esat, T., 2000. The coral record of last interglacial sea levels and sea surface temperatures. Chem. Geol. 169, 107–129.
Mejdahl, V., 1979. Thermoluminescence dating: beta-dose attenuation in quartz grains. Archaeometry 21, 61–72.
Milnes, A.R., Kimber, R.W., Phillips, S.E., 1987. Studies of calcareous aeolian landscapes of Southern Australia. In: Liu, T. (Ed.), Aspects of Loess Research. China Ocean Press, pp. 130–139.
Muhs, D.R., 1992. The last interglacial–glacial transition in North America: evidence from uranium-series dating of coastal deposits. In: Clark, P.U., Lea, P.D. (Eds.), The Last Interglacial–Glacial Transition in North America. USGS, Boulder, Colorado, pp. 31–52. Geological Society of America Special Paper 270.
Muhs, D.R., Skipp, G., Schumann, R.R., Johnson, D.L., McGeehin, J.P., Beann, J., Freeman, J., Pearce, T.A., Rowland, Z.M., 2009. The origin and paleoclimatic significance of carbonate sand dunes deposited on the California Channel Islands during the Last Glacial period. In: Damiani, C.C., Garcelon, D.K. (Eds.), Proceedings of the 7th California Islands Symposium. Institute for Wildlife Studies, Arcata, California, pp. 3–14.
Muller, G., Gastner, M., 1971. The "Karbonate Bombe" a Simple Device for the Determination of the Carbonate Content in Sediments, Soils and Other Materials. Monatshefte. In: Neues Jahrbuch fur Mineralogie, vol. 10, pp. 466–469.
Murray, A.S., Marten, R., Johnson, A., Martin, P., 1987. Analysis for naturally occurring radionuclides at environmental concentrations by gamma spectrometry. Radioanal. Nucl. Chem, 263–288. Articles 115.
Murray-Wallace, C.V., 2002. Pleistocene coastal stratigraphy, sea-level highstands and neotectonism of the southern Australian passive continental margin – a review. J. Quat. Sci. 17 (5–6), 469–489.
Murray-Wallace, C.V., Kimber, R.W.L., 1989. Quaternary marine aminostratigraphy: Perth Basin, western Australia. Aust. J. Earth Sci. 36, 553–568.
Murray-Wallace, C.V., Brooke, B.P., Cann, J.H., Belperio, A.P., Bourman, R.P., 2001. Whole rock aminostratigraphy of the Coorong Coastal Plain, South Australia: towards a 1 million year record of sea-level highstands. J. Geol. Soc. Lond. 158, 111–124.
Nathan, R.P., Mauz, B., 2008. On the dose-rate estimate of carbonate-rich sediments for trapped charge dating. Radiat. Meas. 43, 14–25.
Nicholas, W.A., Borissova, I., Radke, L., Tran, M., Bernardel, G., Jorgensen, D., Siwabessy, J., Carroll, A., Whiteway, T., 2013. Seabed Environments and Shallow Geology of the Vlaming Sub-Basin, Western Australia – Supporting Investigation for Geological Storage of CO_2. Geoscience Australia Record 2013/009. In: Geoscience Australia. Canberra, 82 pp.
Nichol, S.L., Brooke, B.P., 2011. Shelf habitat distribution as a legacy of Late Quaternary marine transgressions: a case study from a tropical carbonate province. Cont. Shelf Res. 31, 1845–1857.
Olley, J.M., Pietsch, T., Roberts, R.G., 2004a. Optical dating of Holocene sediments from a variety of geomorphic settings using single grains of quartz. Geomorphology 60, 337–358.
Olley, J.M., De Deckker, P., Roberts, R.G., Fifield, L.K., Hancock, G., 2004b. Optical dating of deep-sea sediments using single grains of quartz: comparison with radiocarbon ages and implications for the marine carbon reservoir. Sediment. Geol. 169, 175–189.
Petherick, L., Bostock, H., Cohen, T.J., Fitzsimmons, K., Tibby, J., Fletcher, M.-S., Moss, P., Reeves, J., Mooney, S., Barrows, T., Kemp, J., Jansen, J., Nanson, G., Dosseto, A., 2013. Climatic records over the past 30 ka from temperate Australia – a synthesis from the Oz-INTIMATE workgroup. Quat. Sci. Rev. 74, 58–77.
Playford, P.E., 1988. Guidebook to the Geology of Rottnest Island. Geological Society of Australia and Geological Survey of Western Australia, Perth, 67 p.
Playford, P.E., 1997. Geology and hydrogeology of Rottnest Island, Western Australia. In: Vacher, L.H., Quinn, T.M. (Eds.), Geology and Hydrogeology of Carbonate Islands, Developments in Sedimentology, vol. 54. Elsevier, Amsterdam, pp. 783–810.
Playford, P.E., Cockbain, A.E., Lowe, G.H., 1976. Geology of the Perth Basin, Western Australia. In: Bulletin of the Geological Survey of Western Australia, p. 124.
Playford, P.E., Cockbain, A.E., Berry, P.F., Roberts, A.P., Haines, P.W., Brooke, B.P., 2013. Geology of Shark Bay. In: Bulletin 146 of the Geological Survey of Western Australia, 280 p.
Porat, N., Botha, G., 2008. The luminescence chronology of dune development on the Maputaland coastal plain, southeast Africa. Quat. Sci. Rev. 27, 1024–1046.
Prescott, J.R., Hutton, J.T., 1994. Cosmic ray contributions to dose rates for luminescence and ESR dating: large depths and long-term time variations. Radiat. Meas. 23, 497–500.
Price, D.M., Brooke, B.P., Woodroffe, C.D., 2001. Thermoluminescence dating of eolianites from Lord Howe Island and south-west Western Australia. Quat. Sci. Rev. (Quat. Geochronol.) 20, 841–846.
Ramsay, P.J., 1994. Marine geology of the Sodwana Bay shelf, southeast Africa. Mar. Geol. 120, 225–247.
Rivers, J.M., James, N.P., Kyser, T.K., Bone, Y., 2007. Genesis of palimpsest cool-water carbonate sediment on the continental margin of southern Australia. J. Sediment. Res. 77, 480–494.
Roberts, R.G., Galbraith, R.F., Yoshida, H., Laslett, G.M., Olley, J.M., 2000. Distinguishing dose populations in sediment mixtures: a test of single-grain optical dating procedures using mixtures of laboratory-dosed quartz. Radiat. Meas. 32, 459–465.
Roy, P.S., Cowell, P.J., Ferland, M.A., Thom, B.G., 1994. Wave-dominated coasts. In: Carter, R.W.G., Woodruffe, C.D. (Eds.), Coastal Evolution: Late Quaternary Shoreline Morphodynamics. Cambridge University Press, pp. 33–86.
Shulmeister, J., Goodwin, I., Renwick, J., Harle, K., Armand, L., McGlone, M.S., Cook, E., Dodson, J., Hesse, P., Mayewski, P., Curran, M., 2004. The southern hemisphere westerlies in the Australasian sector during the last glaciation cycle: a synthesis. Quat. Int. 118/119, 23–53.
Siddall, M., Chappell, J., Potter, E.K., 2006. Eustatic sea level during past interglacials. In: Sirocko, F., Claussen, M., Sanchez Goni, M.F., Litt, T. (Eds.), The Climate of Past Interglacials. Elsevier, Amsterdam, pp. 74–92.
Sivan, D., Porat, N., 2004. Evidence from luminescence for Late Pleistocene formation of calcareous aeolianite (kurkar) and paleosol (hamra) in the Carmel Coast, Israel. Palaeogeogr. Palaeoclimatol. Palaeoecol. 211, 95–106.
Sprigg, R.C., 1979. Stranded and submerged sea-beach systems of southeast south Australia and the aeolian desert cycle. Sediment. Geol. 22, 53–96.
Spooner, M.I., De Deckker, P., Barrows, T.T., Fifield, L.K., 2011. The behaviour of the Leeuwin Current offshore NW Australia during the last five glacial–interglacial cycles. Glob. Planet. Change 75, 119–132.
Stirling, C.H., Esat, T.M., McCulloch, M.T., Lambeck, K., 1995. High-precision U-series dating of corals from Western Australia and implications for the timing and duration of the Last Interglacial. Earth Planet. Sci. Lett. 135, 115–130.
Stirling, C.H., Esat, T.M., Lambeck, K., McCulloch, M.T., 1998. Timing and duration of the Last Interglacial: evidence for a restricted interval of widespread coral growth. Earth Planet. Sci. Lett. 160, 745–762.
Stokes, S., Ingram, S., Aitken, M.J., Sirocko, F., Anderson, R., Leuschner, D., 2003. Alternative chronologies for Late Quaternary (Last Interglacial – Holocene) deep sea sediment via optical dating of silt-size quartz. Quat. Sci. Rev. 22, 925–941.
Szabo, B.J., 1979. Uranium-series age of coral reef growth on Rottnest Island, Western Australia. Mar. Geol. 29, M11–M15.
Vacher, H.L., Hearty, P.J., Rowe, M.P., 1995. Stratigraphy of Bermuda: nomenclature, concepts, and status of multiple systems of classification. In: Curran, H.A., White, B. (Eds.), Terrestrial and Shallow Marine Geology of the Bahamas and Bermuda. Geological Society of America, Boulder, Colorado, pp. 271–294. Geological Society of America Special Paper 300.
Vacher, H.L., Rowe, M.P., 1997. Geology and hydrogeology of Bermuda. In: Vacher, H.L., Quinn, T.M. (Eds.), Geology and Hydrogeology of Carbonate Islands, Development in Sedimentology, vol. 54. Elsevier, H. L. Amsterdam, pp. 35–90.
Wyrwoll, K.-H., Greenstein, B.J., Kendrick, G.W., Chen, G.S., 2009. The palaeoceanography of the Leeuwin Current: implications for a future world. J. R. Soc. West. Aust. 92, 37–51.
Zhou, L., Williams, M.A.J., Peterson, J.A., 1994. Late Quaternary aeolianites, palaeosols and depositional environments on the Nepean Peninsula, Victoria, Australia. Quat. Sci. Rev. 13, 225–239.